universität wien

MASTERARBEIT / MASTER'S THESIS

Titel der Masterarbeit / Title of the Master's Thesis

„Regulation and Dynamics oft he Nucleoplasmic Pool of A-type Lamins“

verfasst von / submitted by

Konstantina Georgiou

angestrebter akademischer Grad / in partial fulfilment of the requirements for the degree of

Master of Science (MSc)

Wien, 2018 / Vienna 2018

Studienkennzahl lt. Studienblatt / degree programme code as it appears on the student record sheet:	A 066 834
Studienrichtung lt. Studienblatt / degree programme as it appears on the student record sheet:	Masterstudium Molekulare Biologie
Betreut von / Supervisor:	Univ.-Prof. Dr. Roland Foisner

Summary

The nuclear lamina is a filamentous meshwork opposing the inner nuclear membrane of metazoan cells. It provides mechanical support to the nucleus and is involved in a plethora of cellular activities, such as nuclear mechanosignaling and chromatin organization. A- and B- type lamins are the major components of the lamina. B-type lamins remain permanently farnesylated and membrane-associated, while A-type lamins, due to additional post-translational processing and removal of the farnesyl residue, can also be found as a more soluble and dynamic pool in the nucleoplasm. The emerging unique functions of intranuclear lamins prompted us to address remaining open questions regarding their regulation and dynamics during the cell cycle.

First, we investigated the origin and dynamics of nucleoplasmic A-type lamins using ectopically expressed EGFP-pre-lamin A and live-cell imaging. By analyzing changes in the distribution of newly synthesized wild type pre-lamin A and an assembly-deficient lamin A- ΔK32 mutant, both presumable farnesylated, we show that newly expressed farnesylated constructs are rapidly recruited to the nuclear periphery initially, even when they are unable to assemble into the lamina, before they partially, or completely, in the case of mutant lamin A, translocate to the nucleoplasm. In contrast, the fully processed lamin variants lacking farnesylation are localized exclusively in the nucleoplasm in early G1-phase following post-mitotic nuclear reassembly and, unlike the assembly-deficient lamin A- ΔK32 mutant, the majority of wildtype lamin A translocates to the nuclear periphery throughout G1. These data show that both transient lamin A farnesylation and its assembly into the lamina contribute to peripheral localization of lamin A, but these events take place at different cell cycle stages and depend on the processing state of lamins.

Secondly, we investigated the role of the nucleoplasmic lamin A/C-binding protein, lamin associated polypeptide 2 alpha (LAP2α), in the regulation of lamin A localization. Direct monitoring of ectopic EGFP-tagged lamin A throughout G1, and endogenously tagged mEos3.2-lamin A/C in G1, S and G2 phase in LAP2α wildtype and knockout cells revealed no changes in the distribution of intranuclear lamins in the absence of LAP2α. However, we find that antibody staining of nucleoplasmic A-type lamins as well as their solubility and mobility is significantly reduced in LAP2α-depleted cells. Based on these data, we propose a revised model of LAP2α-mediated regulation of the nucleoplasmic lamin A/C pool. We suggest that LAP2α does not influence the level of nucleoplasmic lamins, but rather maintains them in a soluble and dynamic pool, possibly by affecting the assembly state of intranuclear lamins.

Acknowledgement

First and foremost, I would like to express my sincere appreciation to my advisor, Professor Roland Foisner, for giving me the opportunity to carry out my master's thesis in his group. I am deeply grateful for his guidance, encouragement and support throughout this research project.

I would like to thank my supervisor, Dr. Nana Naetar, for being an excellent and extremely patient teacher. I am grateful for her insights, trust, support, enthusiasm and above all, her never-ending positivity. For the warm welcome and wonderful environment, I would like to thank all the lab members, Simona, Christina, Christian, Petra, Selma, Sandra, Azra and Laura. I enjoyed spending time with all of you, learning from you and I could not be more grateful for all the chocolate, coffee, singing and dancing. Looking forward to more of it!

Furthermore, I would like to thank my friends Naya, Christina, Katia, Tonia, Tanja, Nachicho, Andres, Evi, Nico, Queralt, Jakob, Elena, and Borja for their immense tolerance during stressful times and for being my second family in Vienna.

Finally, I owe my deepest gratitude to my family for their love and endless support in every step of the way. Μανούλα, none of this would be possible without you.

Table of Contents

1. Introduction

1.1 The eukaryotic nucleus

The most distinctive feature of eukaryotic cells in comparison to prokaryotic cells is the compartmentalization of cellular processes. For this purpose, eukaryotes possess a diverse range of membrane-enclosed organelles with specific functions. Cellular processes are carried out in a segregated, but well-orchestrated manner within different compartments and synergistically result in a response to innate cellular needs or environmental changes[1]. In prokaryotes, which lack membrane-enclosed organelles, such activities are dispersed within the cytoplasm.

One of the most important organelles in eukaryotic cells is the nucleus, which is acting as the command center of the cell. It contains the majority of the cell's genetic information and controls fundamental biological activities[1]. The nucleus is enclosed by the nuclear envelope, which spatially separates the nucleus from the cytoplasm and facilitates the regulated bidirectional trafficking between the two compartments[2]. The nucleus possesses an intricate and dynamic network of filaments and proteins, called the nucleoskeleton, which establishes a connection of the nucleus to the cytoskeleton and is highly significant for the mechanical support of the nucleus as well as chromatin organization and cellular signaling[3-4]

Eukaryotes are bigger and more complex organisms than prokaryotes and so is their genetic material. Histones bind to eukaryotic DNA to form nucleosomes, the building blocks of higher order chromatin structures, resulting in the tight packaging of the large linear genome into the nucleus in the form of chromosomes[1]. The position of chromosomes within the nucleus is not random; chromosomal domains are organized with great accuracy in relation to each other and to other nuclear components and it has been shown that this localization greatly influences gene expression[5-6]. Zooming in to how single chromosomes are organized, it is possible to distinguish topologically associated domains (TADs)[7], where certain genomic regions interact with each other in much higher frequency than with those outside the domain. It is believed that TADs are independently regulated and genes within a domain display coordinated activity[6]. Disruption of these three-dimensional structures is linked to pathologies owing to modified gene regulation[8], proving that spatial organization of chromatin in the nucleus is crucial for the cellular fate and survival.

1.2 Nuclear Envelope

In metazoan cells the nuclear DNA is enclosed by a double membrane, the nuclear envelope (NE), which creates a nucleocytoplasmic barrier, separating nuclear activities (DNA replication, transcription and RNA processing) from cytoplasmic biological processes (translation and metabolism)[1]. The NE consists of two continuous lipid bilayers, the inner nuclear membrane (INM) and the outer nuclear membrane (ONM). The ONM is contiguous with the endoplasmic reticulum (ER) and both share a similar composition of integral proteins. Nevertheless, even though the ONM and INM are also continuous, their protein content is highly divergent[9-10] and disease phenotypes are caused mainly by mutations of INM proteins[11-12].

Nuclear pore complexes (NPCs) are important constituents of the NE and serve as a bridge of communication between the nucleoplasm and cytoplasm. They consist of numerous single proteins, termed nucleoporins (Nups), and are classified among the largest complexes in the cell. NPCs perforate the NE at numerous sites where the INM and ONM merge. Small molecules can diffuse freely through NPCs, while large macromolecules need to be actively transported ensuring a tightly regulated transport of molecules in and out of the nucleus[2, 13]. Apart from their role as gatekeepers, NPCs have several other functions on both sides of the NE. It is believed that the cytoplasmic face of the NPC facilitates the release and initiation of further processing of exported cargo and, due to connections established with the cytoskeleton, NPCs are implicated in the assembly and dynamics of interphase microtubules, as well as intracellular transport of nuclear cargo. There is increasing evidence that intranuclear NPC structures form a network of proteins involved in processes such as gene expression, RNA biogenesis, chromatin organization and mitosis[14].

The nuclear lamina is a structure underlining the INM of the NE (Figure 1), consisting of nuclear lamins and numerous lamin-binding proteins of the INM[15]. This filamentous network was originally studied because it provides mechanical stability for the nucleus and it was believed that this was its main function. However, as it was later discovered, the nuclear lamina is involved in several cellular processes, such as DNA replication and repair, transcription, gene regulation, signaling and cell differentiation, as well as apoptosis[16-19].

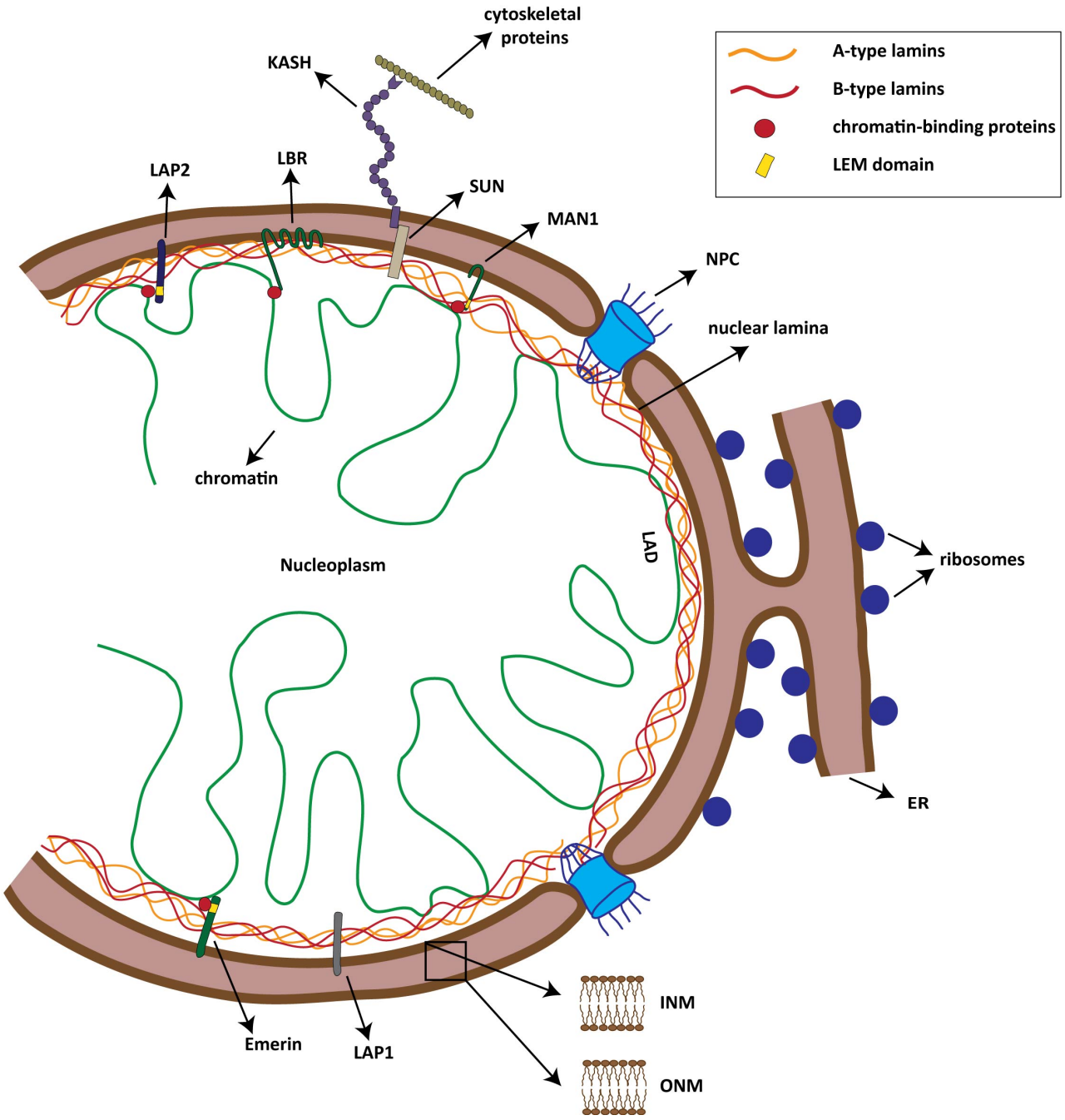

Figure 1. Schematic representation of the major components of the mammalian nuclear envelope. (ER-endoplasmic reticulum; INM-inner nuclear membrane; ONM-outer nuclear membrane; NPC-nuclear pore complex; LAD-lamina associated domain; LEM-LAP2, Emerin, MAN1; LAP1-lamina associate polypeptide 1; LAP2-lamina associated polypeptide 2; LBR-lamin B receptor; SUN-Sad1 and UNC-84 homology; KASH-Klarsicht, ANC-1 and SYNE1 homology).

1.3 Nuclear Lamina

1.3.1 Nuclear lamins

Lamins, the major building blocks of the nuclear lamina, are the only intermediate filament proteins present within the nucleus[20] of metazoan cells and, based on their sequence, they are classified as type V intermediate filaments[21]. It is believed that all intermediate filament proteins derived from a common lamin-like progenitor[22]. Lamins are categorized in two groups, namely A-type and B-type lamins, based on their function, expression profile, biochemical and structural properties[19, 23]. Nuclear lamins are expressed in metazoans, but are not found in unicellular organisms, plants or fungi[24].

At least one form of B-type lamins is expressed in all metazoans. With the exception of *Drosophila melanogaster*, all invertebrate lamins are classified as B-type lamins. Lamin expression in vertebrates is more complex, as, both B-type and A-type lamins are expressed. Vertebrate B-type lamins can be further subdivided into three types, lamins B1, B2 and B3, the latter being expressed exclusively in fish and amphibians. It is believed that B-type lamins are the evolutionary precursors of vertebrate A-type lamins[19]. All A-type lamins are alternative splicing products of the same gene. Four isoforms of A-type lamins have been described: Major isoforms lamin A and C, and minor isoforms lamin C2 and AΔ10.

In mammals, the predominant A-type lamin isoforms, lamin A and lamin C, are encoded by *LMNA*[25], whereas the major B-type lamins, lamin B1 and lamin B2, are encoded by two separate genes, *LMNB1* and *LMNB2*, respectively[26]. The number and type of lamins expressed varies in different organisms, but also among cell types of the same organism. An additional factor influencing the lamin expression of various lamin forms is the developmental stage[26]. B-type lamin expression is independent of the developmental stage; at least one B-type lamin is present in all cells throughout development, whereas A-type lamin expression is developmentally regulated and closely connected with cell differentiation[24].

1.3.2 Inner Nuclear Membrane Proteins

Up to date numerous proteins of the INM have been found to bind to lamins[27-28]. Given that the nuclear envelope transmembrane protein (NET) composition of the INM is tissue and cell type-specific, it is believed that even more lamin-binding proteins are present in metazoan cells, but remain poorly characterized or unverified[29]. According to estimations, more than a hundred proteins interact in a direct or indirect manner with nuclear lamins. The best-characterized proteins among these are: lamin B

receptor (LBR) as well as the lamina-associated polypeptide (LAP) 1, LEM (LAP2, Emerin, MAN1), and SUN-domain groups (Figure 1). Studies on known lamin-binding proteins have described their contribution to nuclear mechanics and architecture as well as to cell-cycle control, signaling and chromatin organization[27].

LBR was the first INM protein identified and shown to be involved in the binding of chromatin to the peripheral lamina and epigenetic silencing of genes[30]. The LAP1 family consists of three isoforms (A, B and C), which have been implicated in neuron signaling and striated muscle maintenance[16]. All proteins of the LEM family are characterized by a common structural motif, the LEM domain, which binds indirectly to chromatin via the Barrier to Autointegration Factor (BAF), a conserved chromatin-, DNA-, and histone-associated protein[31]. LEM proteins have been shown to have a role in chromatin condensation, tethering of heterochromatic regions to the nuclear periphery, nuclear lamina organization, cell differentiation and tissue homeostasis[31]. It has been demonstrated that LEM proteins are involved in the retention of transcription factors at the nuclear lamina, which can exert negative effects on cellular signaling. This, in turn, can influence gene expression, contributing to the function of LEM proteins in several cellular processes[31]. Lastly, the INM SUN (Sad1 and UNC-84 homology) domain proteins establish interactions with ONM proteins containing the KASH (Klarsicht, ANC-1 and SYNE1 homology) domain, resulting in the formation of LINC (Linker of Nucleoskeleton and Cytoskeleton) complexes. Such complexes are involved in nuclear migration, meiosis and they establish a physical link of the nucleoskeleton and cytoskeleton through the interaction of KASH proteins with microtubules, actin and intermediate filaments[16, 27].

1.3.3 Lamin Structure and Assembly

Lamins are intermediate filament proteins and are therefore composed of the typical IF structural domains[32]; a long central rod domain flanked by a globular amino-terminal 'head' domain and a carboxy-terminal 'tail' domain[33-34]. The α-helical rod domain consists of four individual coils, 1A, 1B, 2A and 2B (Figure 2). These segments contain the characteristic heptad repeats (abcdefg) of coiled coil domains (where residues a and d are small hydrophobic amino acids). A linker region, termed L12, separates coils 1 and 2 and is the most flexible of the linker segments. Coils 1A and 2A are separated from 1B and 2B by linkers L1 and L2, respectively[20, 35].

The 'head' domain of lamins is shorter than those found in cytoplasmic IFs and its atomic structure remains a mystery to date. All lamin-specific motifs are located in the 'tail' domain. First,

lamins contain a motif that resembles an Immunoglobulin (Ig)-fold domain, which in humans is known to fold in a typical manner resulting in the formation of two β-sheets[36-37]. Between coil 2B of the central domain and the Ig-fold lies a nuclear localization signal (NLS) necessary for the import of lamins into the nucleus following its translation in the cytoplasm[38]. Finally, all lamins apart from lamin C possess a CaaX motif, where C is a cysteine, a is an aliphatic residue and X is any residue[33-34].

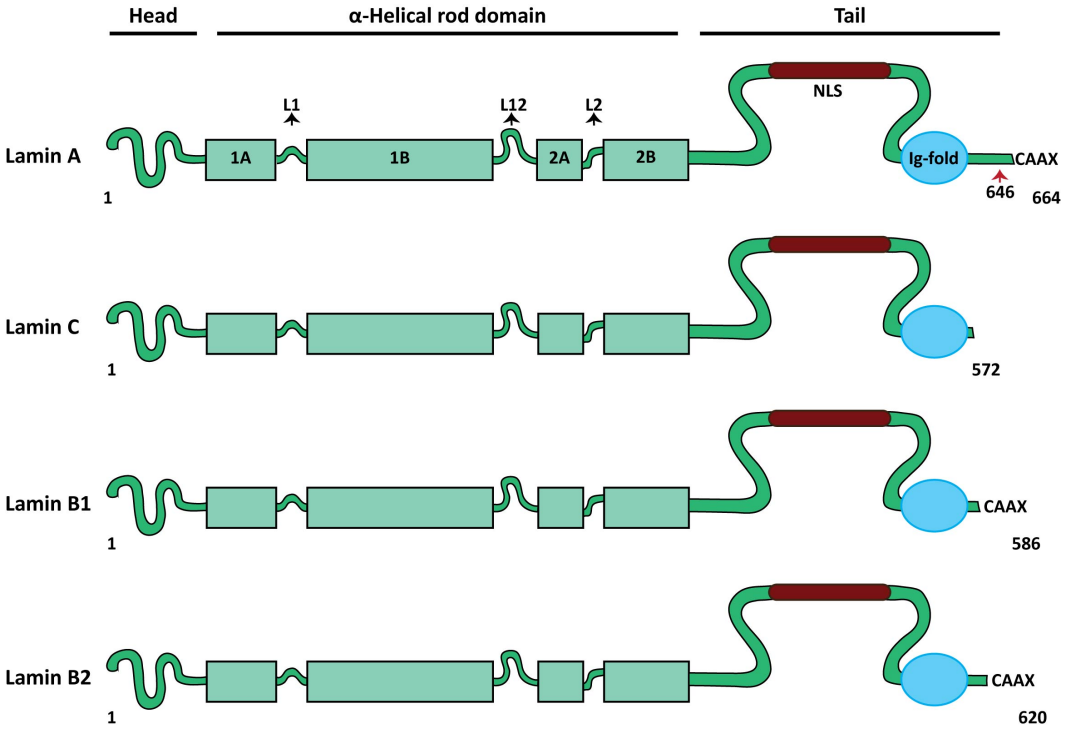

Figure 2. Structure and domain organization of nuclear lamins. Schematic representation of lamin polypeptides consisting of a short N-terminal 'head' domain, a 'central' rod domain and a C-terminal 'tail' domain. The rod domain is separated in four α-helical coils (1A, 1B, 2A, 2B) by linker regions L1, L12 and L2. The carboxy-terminal domain contains a nuclear localization signal (NLS), an Ig-fold and, with the exception of lamin C, a CaaX motif. The length of mature lamin A, following pre-lamin A processing and proteolytic cleavage is indicated by the red arrow.

Deciphering the nuclear lamina structure has been the aim of several scientific studies, but has proven to be a difficult task to accomplish. *In vitro* studies on lamins using electron microscopy have elucidated the initial steps of lamin assembly. Lamins, like most IF proteins, have the tendency to form higher-order assemblies. In the first step, the characteristic α-helical rod domains of two lamin polypeptides are coiled around each other in a parallel manner to form a lamin dimer. Lamin dimers,

which are considered the basic building block of higher-order structures, further elongate to polymers by head-to-tail association. Polar head-to-tail polymers interact laterally in an antiparallel manner to give rise to non-polar protofilaments, which can further assemble into filaments or paracrystalline arrays *in vitro*. These paracrystalline arrays are most likely irrelevant to lamin organization in a biological context as their formation has only been observed in *in vitro* studies[18, 20]. To date, a more detailed *in vitro* assembly model has been proposed only for *Caenorhabditis elegans* lamin (Ce-lamin), which was shown to assemble into stable 10nm-wide filaments. It was suggested that the assembly steps are as follows; lamin dimers form head-to-tail polymers, two of these polymers associate in an antiparallel manner to form a protofilament composed of four molecules. Finally, three or four 5-6nm-wide protofilaments assemble into 10nm intermediate filaments[39].

The first snapshot of the lamin network *in vivo* was obtained using electron microscopy on *Xenopus laevis* oocytes, where lamin B3 (the isoform expressed in amphibian germ lines) appeared to assemble into 10nm filaments organized in a tetragonal fashion[40]. In an effort to gain a better understanding of lamin assembly *in vivo*, Ce-lamin was ectopically expressed in *X. laevis* oocytes, where it was shown to form filaments of approximately 4-6nm in diameter[41]. Similar filaments were detected *in vivo* underlying the INM of *C. elegans* cells, however, confirmation of their lamin identity is still lacking[42]. Variations between *in vitro* and both *ex vivo* and *in vivo* structures could be attributed to interactions with lamin-binding proteins or to post-translational modifications of lamins. It became apparent from this experiment that although the 10nm lamin filaments detected in *Xenopus* are the preferred model of lamina organization, different types of lamins can undergo distinct forms of assembly[18].

It is believed that in mammalian nuclei all lamin isoforms form separate, but interacting networks. Analysis of the distinct lamin A, C, B1 and B2 meshworks revealed that they have highly similar properties and that absence of one isoform, with the exception of lamin B2, alters significantly the supramolecular structure of the other isoforms, therefore indicating that there is interaction between the meshworks[43-44]. A recent study described the high resolution architecture of the lamin meshwork in mammalian cells by cryo-electron microscopy, where lamins were assembled into filaments with a diameter of 3.5nm, which is the estimated diameter of lamin protofilaments[45]. It is still uncertain, whether these filaments represent the physiological structure of lamins in mammalian cells, since the nuclei used in this study were subjected to removal of the vimentin cage and chromatin digestion in order to visualize the lamina.

In summary, over the years, great advances have been made towards resolving the structural organization of the lamina. However, several questions remain open and will likely be subject of further studies in the future.

1.3.4 Lamin Processing

Lamins A, B1 and B2 are produced as pre-lamins and undergo several processing steps to become mature lamins[26, 46-47]. The CaaX motif located at the C-terminus of lamins is a key element for their post-translational modification as it designates a site of farnesylation. The initial farnesylation of the cysteine residue by a farnesyltransferase is followed by a metallopeptidase-mediated (Zmpste24 or RCE1) cleavage of the –aaX residues and a subsequent carboxymethylation of the farnesylated cysteine catalyzed by isoprenylcysteine carboxyl methyltransferase (Icmt)[26, 48-49]. These modifications occur shortly after the production of lamins and it is believed that addition of the highly hydrophobic farnesyl-group facilitates their localization and tethering to the inner nuclear membrane[19, 26]. Interestingly, it has been shown that interference with farnesylation results in inhibition of further post-translational processing, proving that the sequence of modifications is highly significant[46].

Unlike B-type lamins, for which carboxymethylation of the farnesylated cysteine is the final post-translational modification, pre-lamin A, after its recruitment to the nuclear membrane, undergoes another proteolytic cleavage (Fig. 3), catalyzed by the enzyme Zmpste24, causing the removal of 15 amino acids at the C-terminus[50]. This modification results in loss of the farnesyl-group and production of mature lamin A[26]. Since lamin C is lacking a C-terminal CaaX motif[33-34], the aforementioned processing steps are not performed on lamin C. Nevertheless, lamin C is also localized at the nuclear periphery and incorporated in the lamina, suggesting that farnesylation of lamins is not a prerequisite for nuclear lamina targeting[51]. Further evidence to support this hypothesis comes from experiments, where it was shown that inhibition of lamin farnesylation did not interfere with its ability to assemble into the lamina[52]. Treatment of cells with farnesyltransferase inhibitors (FTIs) results in a significant increase in the levels of pre-lamin A that can be found at the nuclear periphery and in the nucleoplasm[53-54]. FTI treatment of cells expressing GFP-fused lamin A lead to accumulation of GFP-pre-lamin A in large nucleoplasmic foci with no apparent incorporation into the nuclear lamina[55]. However, since endogenous pre-lamin A in FTI-treated cells was shown to distribute evenly across the nucleoplasm and the nuclear periphery[54], these foci are most likely due to lamin overexpression and not of biological significance. In summary, all the aforementioned studies demonstrated that inhibition of lamin A farnesylation does not prevent its assembly into the lamina.

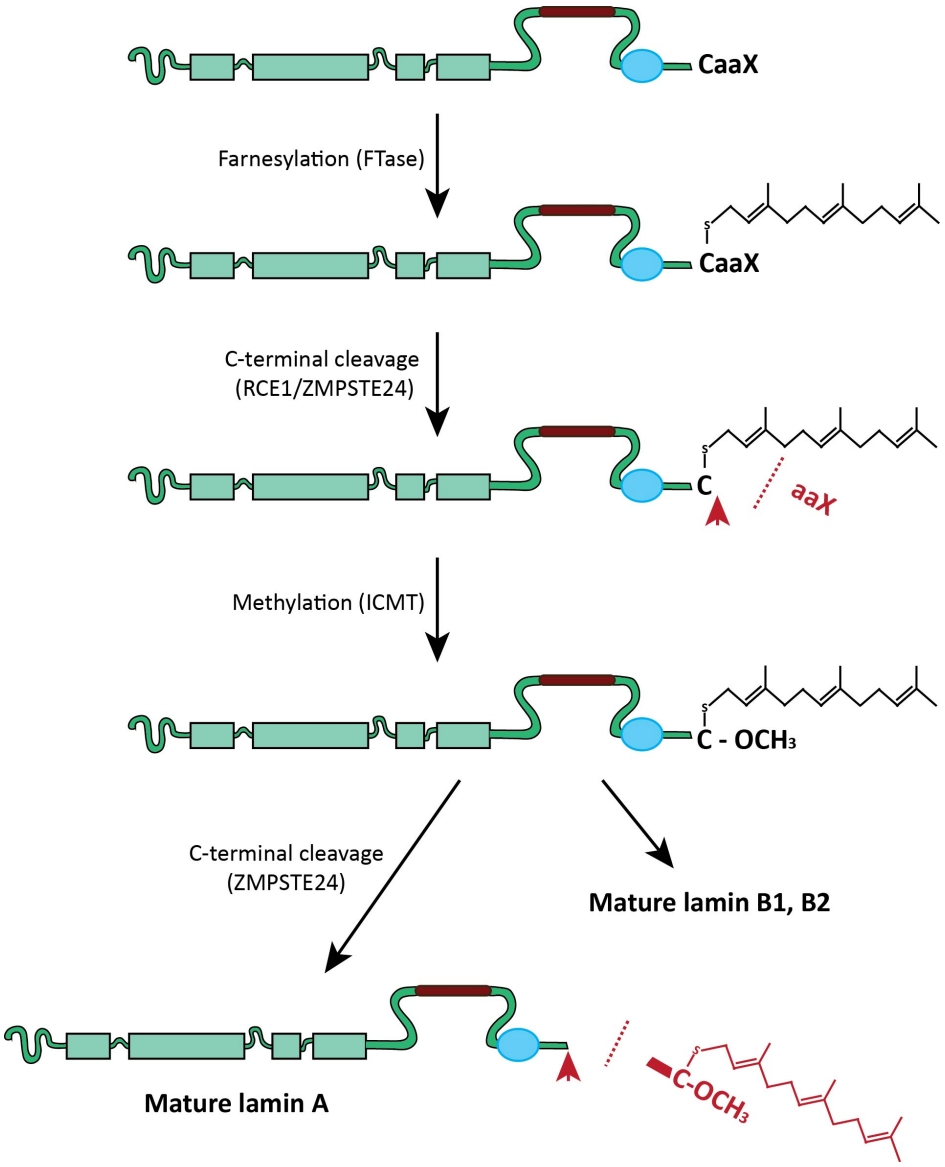

Figure 3. Processing of A-type and B-type lamins. Lamins containing a C-terminal CAAX motif undergo a series of post-translational modifications, which include a farnesylation, a C-terminal cleavage and a carboxy-methylation and yield mature lamin B1 and B2. Production of mature lamin A requires an additional C-terminal cleavage resulting in the removal of the last 15 amino acids and loss of the farnesyl-group. Red arrows indicate cites of proteolytic cleavage. (FTase-farnesyltransferase; RCE1-Ras Converting CAAX Endopeptidase 1; ZMPSTE24-Zinc Metallopeptidase STE24; Icmt-isoprenylcysteine carboxyl methyltransferase).

B-type lamins remain permanently farnesylated and carboxymethylated and therefore are tightly associated with the nuclear membrane throughout the cell cycle. However, lamin A does not retain the farnesyl-group, which is cleaved off during the final processing step yielding mature lamin A and lamin C is never farnesylated[24]. Therefore, mature lamin A and lamin C are less hydrophobic and can, in addition to their localization at the nuclear periphery, also be found in a soluble pool throughout the nucleoplasm.

1.4 Nucleoplasmic lamins

The majority of A-type lamins is incorporated into the lamina; approximately 10% of total lamin A resides in the nucleoplasm. Nucleoplasmic A-type lamins were, for many years, dismissed as a by-product of the lamina or regarded simply as a transient pre-assembly state of lamins. Nevertheless, there is increasing evidence of significant and unique functions carried out by the nucleoplasmic fraction of A-type lamins[56-57].

1.4.1 Structure of intranuclear lamins

Initial electron microscopy studies proposed that lamin filaments are not only present in the peripheral lamina but throughout the nuclear interior[58]. However, using immunostaining or ectopically expressed fluorescently tagged lamins, nucleoplasmic lamins were visualized as an unstructured 'veil'[59], or as distinct intranuclear foci[60].

A small fraction of both A- and B-type lamins is localized within the nucleoplasm. Studies using fluorescence recovery after photobleaching (FRAP)[61-62] and fluorescence correlation spectroscopy (FCS)[60] have demonstrated that A- and B-type lamins integrated into the lamina are virtually immobile. Although intranuclear B-type lamins remain largely immobile, A-type lamins within the nucleoplasm were shown to be considerably more mobile than peripheral lamins (approximately 60% of lamin A is mobile[63]). In fact, FCS detected two fractions of nucleoplasmic A-type lamins with different diffusion coefficients, a fast-moving and a slow-moving fraction[60]. It is unlikely that the estimated molecular masses of these fractions, 1.3MDa (fast) to 2.9GDa (slow), represent exclusively lamins but rather correspond to complexes consisting of lamins and their intranuclear binding partners. Moreover, biochemical extractions of cells with detergent showed that nucleoplasmic A-type lamins were easily extractable under conditions where lamins at the periphery remained more or less insoluble[59, 64].

Although to date the structural properties of intranuclear lamins remain unresolved, data from the aforementioned studies collectively indicate that A-type lamins reside within the nucleoplasm at a lower assembly state than those incorporated in the peripheral lamina, perhaps in the form of short polymers or even lamin dimers.

1.4.2 Regulation of nucleoplasmic A-type lamins

The growing interest in nucleoplasmic lamins raised questions regarding their organization. How is their localization in the nuclear interior regulated? How is a lower assembly state maintained and what prevents the incorporation of this fraction of A-type lamins into the peripheral lamina?

It has been suggested that localization of A-type lamins in the nuclear interior is potentially regulated by post-translational modifications of lamin polypeptides. In addition to the CaaX-dependent modifications, farnesylation and carboxymethylation, lamins can be modified by phosphorylation, sumoylation, non-canonical glycosylation (*O*-GlcNAcylation), acetylation and ubiquitylation[65]. During mitosis the lamina is completely disassembled (discussed below), and it has been demonstrated that phosphorylation of lamins at specific residues flanking both sides of the central rod, Ser22 and Ser392 in human lamin A/C, is required for their disassembly[66]. It has long been hypothesized that phosphorylation of lamins at sites targeted during mitosis and/or distinct, interphase-specific sites could regulate the localization of lamins in the nucleoplasm during interphase as well (Fig. 4). Data supporting this hypothesis derived from a study in which mutated forms of lamin A, modified on Ser22 and Ser392 in order to mimic the phosphorylated protein, were shown to promote the intranuclear localization of lamin A and rendered it easily extractable and highly mobile in interphase[67]. Apart from phosphorylation, sumoylation is the only other post-translational modification shown to influence lamin localization and, potentially the interaction with other proteins carrying the same modification[68]. So far, little is known regarding the effect of the remaining post-translational modifications on the function and regulation of lamins[65].

Intranuclear localization of lamin A/C is also regulated by a member of the LAP2 protein family, namely lamina-associated polypeptide 2 alpha (LAP2α). LAP2α is characterized as one of the non-membrane-bound lamin binding proteins (see below) and binds exclusively to lamin A/C within the nucleoplasm[69]. Cells in which LAP2α has been partially or fully depleted display significantly decreased levels of A-type lamins residing in the nuclear interior and re-introduction of LAP2α expression in deficient cells rescued the nucleoplasmic pool of lamins[59]. Although the mechanism of action remains

unclear, it is believed that LAP2α drives the localization of lamins in the nuclear interior and is involved in maintaining a low assembly state and the stability of nucleoplasmic lamins[56-57].

1.5 Dynamics of peripheral and nucleoplasmic lamins

The amount of nucleoplasmic lamins in a cell varies depending on the cell cycle stage. Cells in S and G2 have relatively low levels of nucleoplasmic lamins, while cells in G1 have the highest content of intranuclear A-type lamins during interphase[57]. This phenomenon is due to the drastic change of lamin dynamics during mitosis.

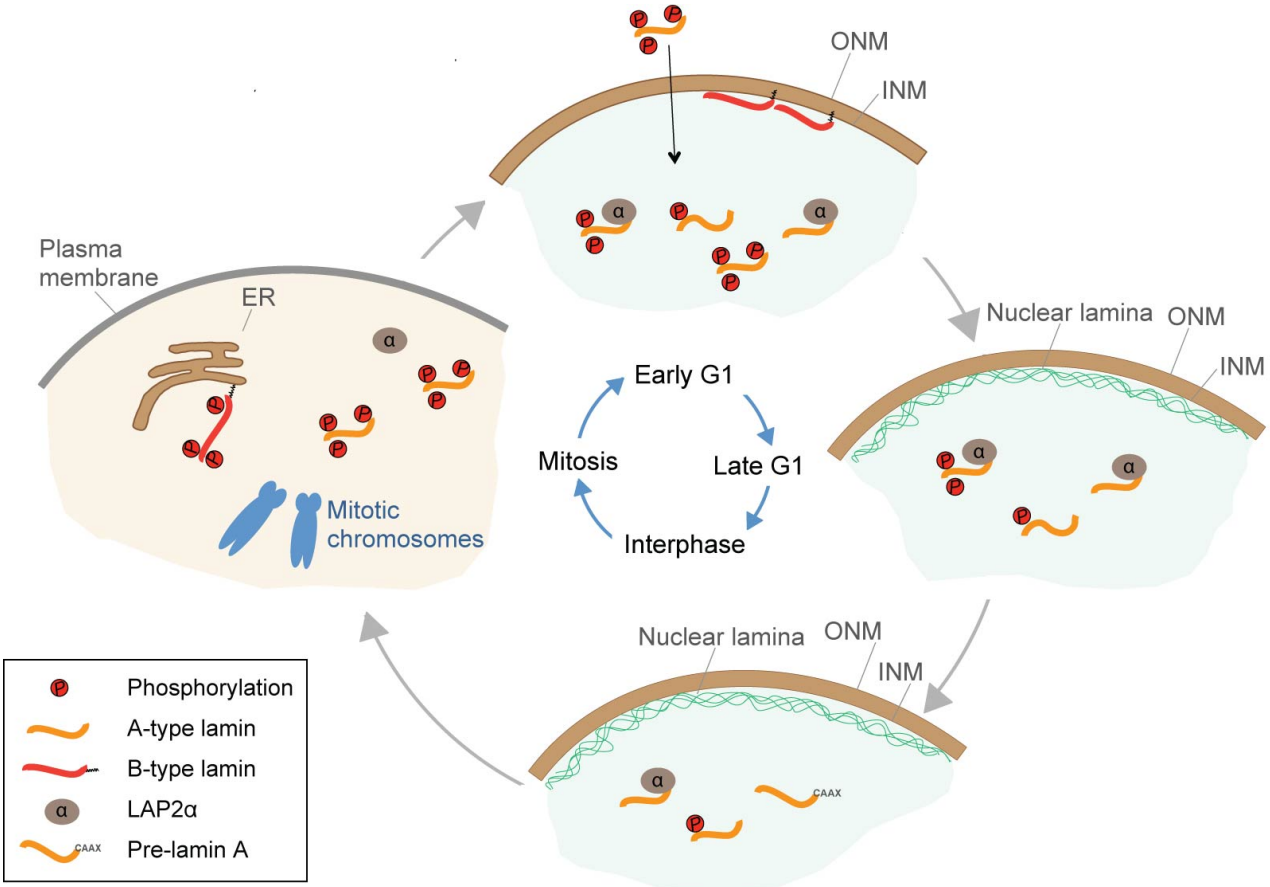

Figure 4. Peripheral and nucleoplasmic lamin dynamics during the cell cycle. Both A- and B-type lamin networks are disassembled in a phosphorylation-dependent manner at the onset of mitosis. Permanently farnesylated B-type lamins remain membrane-bound and localize at the nuclear envelope of newly forming nuclei, while A-type lamins disperse throughout the mitotic cytoplasm and are imported into the nucleus in early G1, initially localize in the nuclear interior and subsequently integrate into the lamina (late G1). A fraction of A-type lamins is prevented from assembling into the lamina and establishes the nucleoplasmic pool of lamins.

The nucleoplasmic pool consists of lamins in a more soluble form, which could be achieved by interphase lamin phosphorylation, LAP2α association and transient localization of nonfarnesylated pre-lamin A in the nucleoplasm (ER-endoplasmic reticulum; INM-inner nuclear membrane; ONM-outer nuclear membrane). Modified from Naetar et al. 2017.

At the onset of mitosis the lamina is disassembled in order to facilitate nuclear envelope breakdown[70]. Phosphorylation of lamins at specific sites flanking the rod domain promotes the depolymerization of the nuclear lamina[66, 71]. After lamina disassembly and breakdown of the nuclear envelope, mature A-type lamins that lack the farnesyl-group are dispersed throughout the cytoplasm of the mitotic cell. On the contrary, B-type lamins retain the farnesyl-group and therefore, remain associated with the nuclear envelope during cell division[72]. Due to their permanent membrane-bound state, at the end of mitosis, while the nucleus is reassembled, B-type lamins are localized at the nuclear envelope and assemble directly into the peripheral lamina. A-type lamins on the other hand, are imported into the newly formed nucleus and, in early G1 phase, localize in the nuclear interior in a soluble pool before gradually assembling into the lamina throughout G1[73]. As A-type lamins assemble into the lamina while the cell cycle progresses, a fraction of this soluble pool remains soluble within the nucleoplasm (Fig. 4).

The dynamic behavior of lamins during cell division is one of the potential sources of the nucleoplasmic pool of lamins. It has been hypothesized that, during G1, when intranuclear A-type lamins originating from the preceding mitosis are integrated into the lamina, a fraction of mature lamin A and lamin C is, by an unknown mechanism, prevented from polymerizing and assembling into the lamina[56-57]. Other possible explanations regarding the origin of nucleoplasmic A-type lamins include the contribution of unprocessed pre-lamin A, which is suggested to transiently localize in the nuclear interior prior to its processing and recruitment to the periphery, and the dynamic exchange of lamins between the peripheral lamina and the nucleoplasmic pool during interphase[57].

1.6 Soluble lamin-binding proteins

Aside from the previously described membrane-bound lamin-binding proteins, lamins located at the nuclear periphery and throughout the nucleoplasm can also interact with soluble nuclear proteins. These include chromatin associated proteins such as BAF and histones, the retinoblastoma protein (pRb), protein kinase C (PKC), sterol regulatory element binding protein (SREBP) 1, c-fos and LAP2α[27].

Interestingly, LAP2α has not only been shown to associate with intranuclear lamins but also to regulate their localization within the nuclear interior[59].

1.6.1 Lamina-associated polypeptide 2 (LAP2) family of proteins

In mammals the LAP2 family of proteins consists of six alternatively spliced isoforms (LAP2 α, β, γ, δ, ε and ζ) encoded by the *LAP2* (*Tmpo*) gene[74]. All LAP2 isoforms consist of a common 187aa-long N-terminal domain and a variable C-terminal domain. Since the common LAP2 N-terminus contains a LEM domain that interacts with chromatin via BAF, LAP2 proteins belong to the LEM domain protein family. All members of the LAP2 family have an additional LEM-like domain at their N-terminus, which directly interacts with DNA[75].

Nearly all splice variants have closely related C-termini and except for LAP2α, all other members of the family are, in fact, shorter variants of LAP2β (Fig. 5). Apart from LAP2 α and ζ, the remaining isoforms contain a transmembrane domain at their C-terminus and are, therefore, integral inner nuclear membrane proteins. LAP2α is one of a kind within its family because it is composed of the LAP2 common N-terminal domain and a unique C-terminal domain[28]. The unique LAP2α C-terminus is responsible for differences in localization, binding partners and function compared to other members of the family.

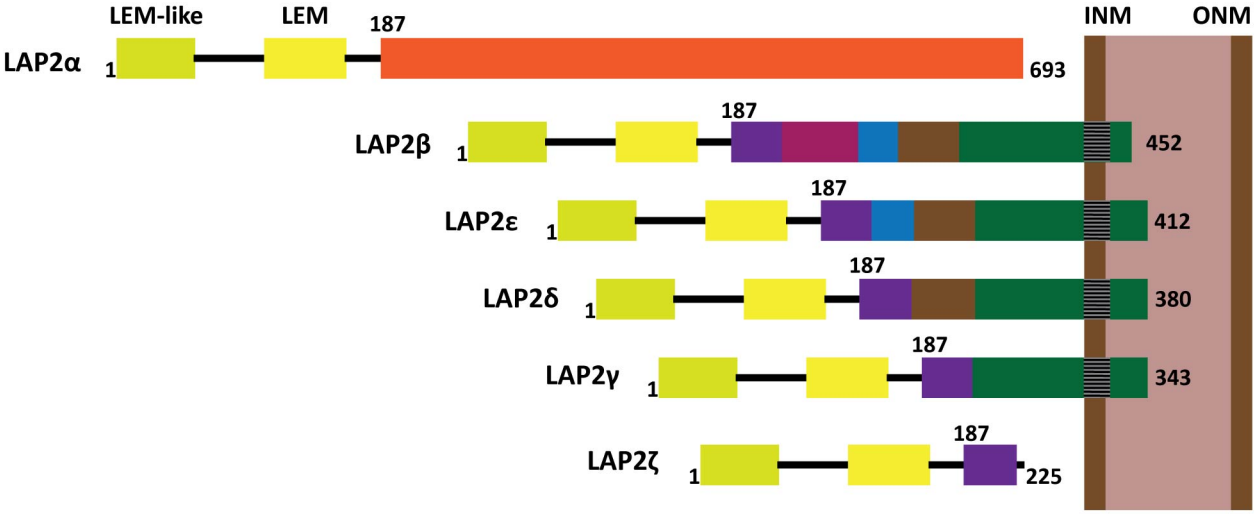

Figure 5. Structural organization of mammalian LAP2 isoforms. The LAP2 common 187aa-long N-terminal domain consists of a LEM and a LEM-like domain. All isoforms apart from LAP2α are closely related structurally and most of them contain a transmembrane domain (grey-black stripped box). The unique C-terminal domain of LAP2α is illustrated in orange (INM-inner nuclear membrane; ONM-outer nuclear membrane).

1.6.2 Lamin-associated polypeptide alpha (LAP2α)

LAP2α is more distantly related to the rest of the LAP2 members due to its unique C-terminal domain. It only shares the LAP2 common N-terminal domain with the other isoforms. The complete C-terminus of LAP2α is encoded by the biggest exon of the LAP2 gene, exon 4. Interestingly, although the *TMPO* gene is present in all vertebrates, exon 4, and therefore LAP2α, has only been identified in mammals and no ortholog of the protein has been detected in fish, amphibians and birds so far[75-76].

The LAP2α-specific C-terminus (Fig. 6) does not contain a transmembrane domain, hence the protein is localized throughout the nucleoplasm[77]. All membrane-bound LAP2 isoforms are known to interact with B-type lamins of the peripheral lamina through their C-termini, however, LAP2α has been shown to exclusively bind A-type lamins located in the nuclear interior via a binding site spanning the last ~80aa of the polypeptide[69]. Apart from the common LEM and LEM-like domains, LAP2α can establish interactions with chromatin through an additional C-terminal chromosome-association domain[78]. Finally, LAP2α has been shown to interact with an important cell cycle regulator protein called retinoblastoma protein (pRb) through an interaction site at its C-terminal tail[79].

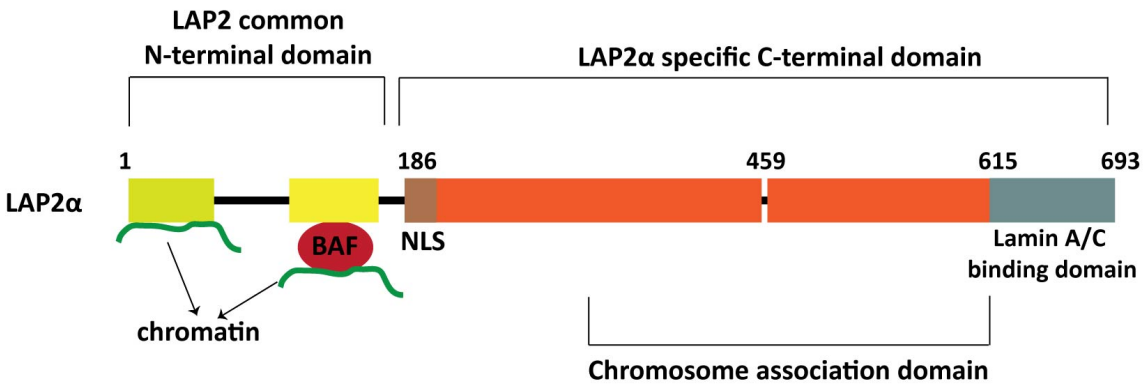

Figure 6. Structural organization and functional domains of LAP2α. LAP2α can interact with chromatin via the LEM and LEM-like domains, as well as the chromosome-association domain of its C-terminus. The LAP2α-specific domain also mediates interactions with nucleoplasmic A-type lamins and pRb (BAF-Barrier to Autointegration Factor; NLS-nuclear localization sequence).

The complete structure of the LAP2α-specific domain has not been fully resolved yet. Based on conserved domains and solved or hypothetical conformations, the α-unique C-terminus is subdivided in two regions. A nuclear localization signal is located at the beginning of the C-terminus and the remaining

segment of the first region is reported as highly disordered. X-ray crystallography has yielded the resolved conformation of the second C-terminal region, which seems to mediate the dimerization of LAP2α[80]. The dimerization domain of each monomer is believed to be comprised of six α-helices, which fold into an anti-parallel four-stranded coiled coil.

1.7 Functions of the nucleoplasmic A-type lamins-LAP2α complex

Considering the ability of LAP2α to bind nucleoplasmic lamins and regulate their localization, in combination with the distinct properties of the mobile and dynamic intranuclear lamin pool, it is interesting to investigate the putative functions of the nucleoplasmic lamin A/C-LAP2α complex.

1.7.1 Regulation of gene expression by lamin A/C and LAP2α

Both, peripheral and nucleoplasmic lamins associate with chromatin and are speculated to regulate gene expression. A- and B- type lamins located at the nuclear periphery interact mainly with gene-poor, heterochromatic regions, termed lamina-associated domains (LADs). Chromatin immunoprecipitation combined with deep sequencing (ChIP-seq) detected interactions of intranuclear A-type lamins both, with heterochromatic and open euchromatic genomic regions[81]. It is believed that interactions with LADs located at the periphery or the interior of the nucleus have a repressive effect on gene expression, while the A-type lamin-mediated regulation of genes in euchromatic regions seems to be more complex. Interestingly, the same euchromatic regions that are bound by lamins A/C are bound by LAP2α. Upon LAP2α depletion, nucleoplasmic lamin A/C chromatin binding is significantly rearranged, including a shift from euchromatic chromatin regions towards repressed heterochromatic LADs[81]. Moreover, there are genome-wide changes in active and repressive epigenetic marks at regions, where lamin A/C binding is lost upon LAP2 depletion. Taking into consideration these results, it was hypothesized that nucleoplasmic lamins and LAP2α regulate gene expression by altering epigenetic pathways[57]. Implication of nuclear lamins in gene expression regulation was further supported by data suggesting that during adipocyte differentiation lamin A/C binding to specific promoters is involved in repression of differentiation-related genes[82].

1.7.2 A-type lamins and LAP2α in mitosis

Another common function that has been proposed for both A-type lamins and LAP2α is their involvement in nuclear envelope reassembly following mitosis. Although the contribution of lamins

during this process is not clear, reassembly of A-type lamins around the decondensing chromosomes of post-mitotic nuclei suggests a role of lamin A/C in nuclear envelope reassembly[83]. In line with this suggestion, it was shown that when a disease-variant of A-type lamins is expressed, cells display defects in cell division; including delayed nuclear assembly[73]. During mitosis, LAP2α has been shown to bind telomeric regions of condensed chromosomes[72]. It is hypothesized that this interaction is established through the chromosome association domain in the LAP2α-specific C-terminus[84] and is regulated by Cdk1-mediated phosphorylation, since all Cdk1 sites identified in LAP2α overlap with this domain[85]. In fact, mutations interfering with the phosphorylation of these sites resulted in the re-localization of LAP2α from telomeric regions to all around mitotic chromosomes. Impaired phosphorylation, however, was not sufficient to block reassembly of the nuclear envelope. Surprisingly, nuclear reassembly was inhibited by overexpression of a variant of the LAP2α C-terminus lacking the LEM and LEM-like domains[84], suggesting that these domains could also possibly mediate the association with mitotic chromosomes.

1.7.3 Nucleoplasmic lamins-LAP2α complex and cell-cycle control

Implication of lamin A/C-LAP2α complexes in the regulation of cell-cycle control was suggested after it was revealed by i*n vivo* and *in vitro* studies that A-type lamins and their binding partner, LAP2α, both bind to the retinoblastoma protein (pRb)[75, 79, 86]. This tumor suppressor protein is a major cell-cycle regulator; it has a pivotal role during the G1 phase checkpoint, where it blocks S phase entry and cell cycle progression. Inhibition of G1 to S phase transition is achieved by binding of E2F transcription factors by pRb, inhibiting in this way transcription of E2F-target genes and subsequently proliferation[87]. pRb activity, itself, is controlled via phosphorylation. In fact, only hypo-phosphorylated pRb binds E2F transcription factors, and its phosphorylation triggers E2F release and cell cycle progression.

Results of several studies investigating the effect of A-type lamins on pRb function have collectively shown that binding by A-type lamins influences pRb activity and/or stability by preventing its degradation[88], promoting pRb dephosphorylation[89] and maintaining its hypo-phosphorylated state[90]. Data supporting a combined role of A-type lamins and LAP2α in the regulation of pRb comes from a study where LAP2α-deficient mice displayed an increased proliferation rate of tissue progenitor cells coupled with loss of nucleoplasmic A-type lamins and deregulation of the pRb pathway[59]. Moreover, knock down of LAP2α was shown to promote proliferation[59], whereas its overexpression reduces it[79].

1.8 Lamins and disease

Mutations in lamin genes are accountable for a group of rare genetic disorders termed laminopathies. A surprisingly high number of over 400 disease-inducing mutations have been described to date in the LMNA gene alone. However, very few disease-causing mutations in LMNB1 and LMNB2 have been described, possibly because mutations in B-type lamins result in severe phenotypes and are lethal[91].

Laminopathies display a variety of symptoms and they can be broadly categorized into four different disease groups based on the tissues they affect[92]. The first, and most prominent, group of laminopathies includes syndromes that affect cardiac and skeletal muscles, such as Emery-Dreifuss muscular dystrophy (EMDM) and dilated cardiomyopathy (DCM). The second group consists of metabolic diseases and diseases affecting adipose tissue, including Dunnigan-type familial partial lipodystrophy (FPLD) and the metabolic syndrome (MS). The third group of laminopathies is comprised of peripheral neuropathies, for instance Charcot-Marie-Tooth disease (CMT). Finally, the last group of laminopathies affects multiple tissues and consists of premature ageing syndromes, the most prominent being Hutchinson Gilford Progeria Syndrome (HGPS)[92].

Apart from lamin mutations, defects in genes encoding for lamin-binding proteins have also been linked with diseases, causing phenotypes similar to laminopathies[12]. Several mutations of the emerin gene give rise to an X-linked form of EMDM and defects in LAP2α are linked to DCM. However, not all diseases caused by mutations in lamin-binding proteins resemble laminopathies. Mutations in LAP1, MAN1 and LBR are linked to primary dystonia, Buschke-Ollendorff syndrome and Pelger–Huet anomaly (PHA) respectively[28].

Although the underlying molecular mechanisms of laminopathies are not entirely clear, three main models were suggested in an attempt to explain the broad range of diseases caused mainly by mutations within a single gene, *LMNA*[18, 57, 92]. According to the "mechanical" model, certain disease-linked lamin variants compromise the structural stability or assembly of the nuclear lamina. Due to the connection between the nucleoskeleton and cytoskeleton via LINC complexes, destabilization of the lamina can render the cells less resistant to mechanical stress and overall more fragile[93-94]. The "gene expression" model proposes that mutations in *LMNA* interfere with the chromatin organization properties of A-type lamins, resulting in misregulation of tissue-specific gene expression[16]. Lastly, the third model is based on the finding that A-type lamins, and their binding partner LAP2α, interact with

the cell cycle regulator pRb. Moreover, A-type lamins interact with another important regulator of cell cycle progression, cyclin D3[95]. Therefore, the "cell proliferation and differentiation"[96] model suggests that mutant forms of A-type lamins induce differentiation and proliferation defects and impair tissue homeostasis.

1.9 Aim of this study

The peripheral lamina has been the subject of numerous studies over the years due to its implication in a vast variety of cellular processes. On the other hand, intranuclear lamins have not been as extensively studied and many questions remain open. Alongside the relative recent description of unique and important functions of nucleoplasmic A-type lamins, distinct from those fulfilled by the lamina, the need to gain a better understanding of the nucleoplasmic lamin pool has become increasingly apparent. The aim of this study was to investigate the origin, dynamics and regulation of nucleoplasmic A-type lamins.

During this study, we first examined putative sources of nucleoplasmic lamins by monitoring ectopically expressed EGFP-tagged lamin A in post-mitotic nuclei using live cell imaging. During mitosis, the peripheral lamina completely disassembles and all the A-type lamins are transiently found in the nucleoplasm. By following individual cells over time, we were trying to see whether, how, and when these disassembled lamins contribute to the nucleoplasmic lamin pool. Furthermore, we tracked cells expressing newly synthesized premature and mature forms of lamin A, as well as lamin A-ΔK32, a mutant variant of lamin A displaying assembly defects, in order to investigate whether newly synthesized lamins A/C can also contribute to the nucleoplasmic lamin pool, in this case without the need of an interjacent mitosis.

The second part of this study is focused on the LAP2α-mediated regulation of nucleoplasmic lamins. Our lab has previously found that LAP2α exclusively interacts with intranuclear lamin A/C[69]. Moreover, we found that cells from LAP2α knockout mice displayed reduced levels of nucleoplasmic A-type lamins in immunofluorescence studies[59], suggesting that LAP2α is a crucial regulator of the nucleoplasmic pool of A-type lamins. However, it remained unclear how exactly LAP2α regulates A-type lamins. Is it, for example, involved in the formation of the intranuclear lamin pool, or is it, possibly, required to keep lamins in the nuclear interior throughout the cell cycle? To address these questions, we studied the distribution of ectopically expressed lamin A, as well as endogenously tagged lamin A/C during different cell cycle stages in LAP2α knockout and control cells. Finally, we attempted to elucidate the molecular mechanisms of this LAP2α-dependent regulation of nucleoplasmic A-type lamins by studying lamin solubility and phosphorylation levels in the absence and presence of LAP2α.

2. Materials and Methods

2.1 Materials

2.1.1 Buffers and Solutions

Harvesting buffer: PBS (Sigma Aldrich), 1xProtease Inhibitors (Roche - cOmplete, EDTA-free), 1mM EDTA (Invitrogen - 0.5M, pH 8.0)

High salt RIPA buffer: 25mM Tris-HCl pH 7.6, 500mM NaCl, 1% NP-40, 1% Sodium Deoxycholate, 0.1% SDS

Lysis buffer: high salt RIPA buffer, 2xProtease Inhibitors (Roche - cOmplete, EDTA-free), 1mM EDTA (Invitrogen - 0.5M, pH 8.0), 1:100 Phosphatase Inhibitor cocktail 2 and 3 (Sigma Aldrich)

Sample buffer (3x): 186mM Tris pH 6.8, 30% Glycerol, 6%SDS, 300mM DTT, 0.1% Bromophenolblue

Extraction buffer: 20mM Tris-HCl (pH=7.5), 150mM NaCl, 2mM $MgCl_2$, 0.5% NP-4O, 1mM DTT, 1U/ml benzonase, 1mM phenylmethylsulfonyl fluoride (PMSF), 1xProtease Inhibitors (Roche - cOmplete, EDTA-free), 1:100 Phosphatase Inhibitor cocktail 2 and 3 (Sigma Aldrich)

SDS-page gel:

Reagents (ml)	10% Resolving Gel (25ml)	5% Stacking Gel (10ml)
dH_2O	9,9	6,8
30% Acryl-bisacrylamide mix	8,3	1,7
1,5M Tris (pH 8.8)	6,3	-
1,5M Tris (pH 6.8)	-	1,25
10% SDS	0,25	0,1
10% Ammonium persulfate (APS)	0,25	0,1
TEMED	0,01	0,01

2.2 Methods

2.2.1 Cell Culture

Cell lines

HeLa LAP2α wildtype and knockout cells were routinely maintained in high-glucose DMEM (Sigma Aldrich) supplemented with 10% Fetal Bovine Serum (FCS, Sigma Aldrich, non U.S. product), 2mM L-Glutamine (PAN-Biotech), 100U/ml penicillin and 100µg/ml streptomycin (Sigma Aldrich). Cells were cultivated at 37°C and 5% CO_2 in a humidified incubator. Clones of immortalized LAP2α $^{(+/+)}$ and LAP2α $^{(-/-)}$ mouse dermal fibroblasts (MDFs) as well as mEos3.2-LMNA MDFs were cultivated in the same medium with the addition of non-essential amino acids (GE Healthcare, PAA) and under the same conditions.

Thawing cells

Cryovials containing the frozen cells were placed into a 37°C water bath for 1-2 minutes, transferred to a 15ml falcon tube containing 10ml of medium and centrifuged at 1100rpm for 4 minutes in a Heraeus table top centrifuge. After centrifugation, the supernatant was removed and the pellet containing the cells was resuspended in medium. The resuspended cells were then added to a tissue culture plate containing growth medium.

Passaging of adherent cells

For cell passaging, the medium was discarded from the dish and cells were washed once with Dulbecco's Phosphate Buffered Saline solution (DPBS, Sigma Aldrich). PBS was subsequently removed, Trypsin-EDTA solution (Sigma-Aldrich) was added and the cells were incubated for 2-3 minutes at 37°C. After incubation, trypsin was inactivated by addition of medium and cells were resuspended. Depending on the desired confluency, the correct amount of cell suspension was transferred into a fresh tissue culture dish containing fresh medium and returned to the incubator.

Freezing of cells

Cells were washed with PBS, trypsinized, collected and centrifuged for 4 minutes at 1100rpm in a Heraeus table top centrifuge. The supernatant was discarded and the pellet of a 10cm dish was resuspended in 2ml pure FCS with 10% DMSO (Sigma Aldrich). 1ml of the cell suspension was

transferred to each cryovial (2 cryovials/10cm dish). Finally, the cryovials were placed in a styrofoam box, stored in -80°C overnight and transferred to -150°C.

2.2.2 Polymerase chain reaction (PCR)

Genotyping PCR

Genomic DNA was prepared using QIAGEN's DNeasy Blood and Tissue Kit according to manufacturer's instructions. Genotyping PCR was performed using genomic DNA isolated from LAP2α wildtype and knockout mouse dermal fibroblast clones, derived after CRISPR-Cas9 mediated knock-in of mEos3.2[97] into the *LMNA* locus, to determine the clonal *LMNA* genotype (*LMNA*-wildtype versus knock-in). The following reagents were mixed for the reaction: 40ng of genomic DNA, 1x GoTaq Green Master Mix (Promega), 0.2µM Forward Primer, 0.2µM Reverse Primer and ddH_2O up to 20µl volume per reaction. Primer sequences, primer pairs and product sizes are indicated in Tables 1 and 2.

Genotyping PCR was performed according to the following protocol:

1. Initial denaturation for 2 minutes at 95°C
2. Denaturation at 95°C for 30 seconds
3. Annealing at 57°C for 30 seconds
4. Extension at 72°C for 30 seconds

x35

5. Final extension at 72°C for 5 minutes

2.2.3 High-Fidelity Polymerase Chain Reaction (Hi-Fi PCR)

PCR amplification was performed using Q5 High-Fidelity DNA polymerase (New England BioLabs), to avoid any mutations in the desired regions. The following solutions were added in an Eppendorf tube: 40ng template DNA, 1x Q5 Reaction Buffer, 200µM dNTPs, 0.5µM Forward Primer, 0.5µM Reverse Primer, 0.02units/µl Q5 High-Fidelity DNA Polymerase, and ddH2O up to 20µl volume per reaction. Hi-Fi PCR was used for the amplifications stated below:

Long range (LR-) PCR

LR-PCR was performed using genomic DNA isolated from LAP2α wildtype and knockout mouse dermal fibroblast clones to test for proper 3-prime and 5-prime integration of mEos3.2 at the *LMNA* locus. Primer sequences, primer pairs and product sizes are indicated in Tables 1 and 2.

LR-PCR was performed according to the following protocol:

1. Initial denaturation for 2 minutes at 98°C
2. Denaturation at 98°C for 10 seconds
3. Annealing at 68°C for 30 seconds
4. Extension at 72°C for 2 minutes

x36

5. Final extension at 72°C for 2 minutes

Table 1. Primers used for PCR reactions.

Name	Primer Sequence
Lmna-WT-KI forward	GATCGATGTACACGGCCAGG
Lmna-WT reverse	GTCCTTCTGTCCAAGTCCCG
Lmna-Eos reverse (Lmna-5prime-2 reverse)	GTGGACCACTGCATTGAGATTTT
Lmna-5prime-1 forward	CCCATCTGTGCACATGACCT
Lmna-5prime-1 reverse	GAGCATGCTGTTGCTCATTCT
Lmna-5prime-2 forward	TGGGACTCCTCTAACTTGCCT
Lmna-3prime-1 forward	GGTAACTTGACACCCTTCTCCTTAG
Lmna-3prime-1 reverse	CCTAGGTTCCCTCCCCTAGAT
Lmna-3prime-2 forward	TCTGCATAACTGGACCATTGGC
Lmna-3prime-2 reverse	GTTTGGGATGAAAGCCCTCCT

Table 2. Primers pairs used for PCR reactions.

Primer Pair	PCR	Product size (bp)
Lmna-WT-KI forward & Lmna-WT reverse	Genotyping	213 (WT) 894 (KI)
Lmna-WT-KI forward & Lmna-Eos reverse	Genotyping	250 (KI)
Lmna-5prime-1 forward & Lmna-5prime-1 reverse	LR	1710
Lmna-5prime-2 forward & Lmna-Eos reverse	LR	1875
Lmna-3prime-1 forward & Lmna-3prime-1 reverse	LR	2566
Lmna-3prime-2 forward & Lmna-3prime-2 reverse	LR	2738

2.2.4 SDS Polyacrylamide gel electrophoresis (PAGE) and Immunoblotting

Collection of cells

To prepare the samples for protein extraction, $2x10^6$ cells were plated on a 10cm dish and incubated at 37°C overnight. Subsequently, cells were washed two times with PBS, placed on ice, scraped off the plate in 2ml Harvesting buffer (see Materials) and collected in falcons. The samples were centrifuged at 1200rpm for 4 minutes at 4°C in a Heraeus table top centrifuge, the supernatant was discarded, the pellet was placed on dry ice for 5 minutes and stored at -80°C overnight.

Protein isolation

For protein isolation, the collected cell samples were transferred on ice, resuspended in 150µl Lysis buffer (see Materials) and transferred to eppendorf tubes. The samples were then sonicated at 50% intensity for 3 seconds using the Sonopuls HD 200 sonicator from Bandelin and incubated end-over-end for 30 minutes at 4°C. Following the incubations, the samples were centrifuged at 10000rpm at 4°C for 10 minutes in an eppendorf table top centrifuge, the supernatant was transferred to clean eppendorf tubes and Sample buffer (1:3) was added to the final lysates.

Note: Before the addition of Sample Buffer, 3µl of each lysate were aliquoted in separate eppendorf tubes in order to perform protein quantification.

Protein quantification

Each sample was diluted 1:10 in dH_20 (3µl lysate + 27µl dH_20) and determination of the protein concentration was performed according to the instructions provided by the Pierce BCA Protein Assay Kit (ThermoFisher Scientific) and evaluated using BioTek's Synergy H1 microplate reader.

Western blot

Prior to loading of the samples, proteins were denatured for 5 minutes at 95°C. Samples were loaded on 1mm 10% SDS page gels and separated using the MiniProtean electrophoresis system from Bio-Rad. Following their separation, proteins were transferred to 0.2µm Nitrocellulose Blotting Membrane (GE Healthcare, PAA) using the Mini Trans-blot cell from Bio-Rad and blocked at 4°C overnight with 5% fat-free milk (Roth) in 0.05% Tween/PBS (PBST). The membranes were then washed three times with PBST and incubated with the primary antibody (Table 3) diluted in 2% BSA/PBST +

0.02% NaN_3 overnight at 4°C. After the incubation, membranes were washed three times with PBST and incubated with the secondary antibody diluted in PBST for 1 hour at room temperature. Membranes were washed three times with PBST and visualized using SuperSignal West Pico Chemiluminescencent Substrate (ThermoFisher Scientific) and the ChemiDoc Touch Imaging System by Bio-Rad.

Table 3: List of antibodies used for immunoblotting and immunofluorescence experiments.

Antibody	Origin	Western Blot Dilution	Immunofluorescence Dilution
Lamin A/C (N18 – rabbit polyclonal)	Santa Cruz Biotechnologies	-	1:100
Lamin A/C (E1 - mouse monoclonal)	Santa Cruz Biotechnologies	1:1000	1:100
Lamin A/C (3A6 - mouse monoclonal)	Generated by Egon Ogris at the MFPL Monoclonal Antibody Facility	-	1:100
LAP2α (1H11 - mouse monoclonal)	Generated by Petra Fichtinger at the MFPL	1:1000	1:100
Phosphorylated-Lamin A/C (Ser22 - rabbit polyclonal)	ThermoFisher Scientific	1:200	1:400
Phosphorylated-Lamin A/C (Ser392 - rabbit polyclonal)	Abcam	1:500	1:100
α-actin (I-19 - goat polyclonal)	Santa Cruz Biotechnologies	1:5000	-
γ-tubulin (GTU-88 - mouse monoclonal)	Sigma Aldrich	1:5000	-

2.2.5 Immunofluorescence

Cells were grown on glass coverslips, washed with PBS and fixed with 4% paraformaldehyde in PBS for 10 minutes at room temperature. Fixed cells were washed twice with PBS and incubated with 50mM NH_4Cl in PBS for 5 minutes at room temperature to stop the fixation. Cells were washed twice with PBS and permeabilized with 0.5% Triton X-100 in PBS for 5 minutes at room temperature. Cells were then washed twice with PBS and blocked with 0.2% gelatine in PBS for 30 minutes at room temperature. The coverslips were incubated with the primary antibodies (for detailed list see Table 3) diluted in PBS at room temperature for 1-2 hours and washed three times with PBS. The secondary antibodies were diluted in PBS and the coverslips were incubated at room temperature for 1 hour and washed three times with PBS. Samples were then mounted in VECTASHIELD Antifade Mounting Medium with DAPI (Vector Laboratories) and sealed. The coverslips were stored at 4°C. Imaging of the samples

was performed using an inverse point scanning confocal microscope (Zeiss LSM 710) and 63x objective (Plan-Apochromat 63x/1.4 Oil). Processing of the images was performed in FIJI.

2.2.6 RT-qPCR

RNA isolation

Cells were collected in eppendorf tubes and centrifuged for 4 minutes at 1200 rpm in a Heraeus table top centrifuge. The supernatant was removed and the pellet was washed once with PBS. The cells were centrifuged for additional 4 minutes at 1200 rpm, the supernatant was discarded and the pellet was resuspended in RLT Buffer containing β-mercaptethanol (10µl/1ml buffer). RNA was isolated from the samples following the instructions provided by QIAGEN's RNeasy mini plus kit.

cDNA synthesis

To synthesize cDNA the following reagents were mixed: 500ng of RNA, 0.7µl of 0.5µg/µl Oligo(dT)18 primer and ddH_2O. Samples were incubated at 65^{o}C for 5 minutes and briefly chilled on ice before adding 4µl 5xReaction Buffer, 0.5µl Thermo Scientific Ribolock RNase Inhibitor, 2µl dNTP mix (10mM each) and 1µl RevertAid Reverse Transcriptase (Thermo Scientific). Samples were then incubated for 60 minutes at 42^{o}C and heated at 70^{o}C for 10 minutes to terminate the reaction.

Real time quantitative PCR (RT-qPCR)

RT-qPCR was performed for the genes of interest and a housekeeping gene. PCR amplification was performed in triplicates with KAPA SYBR Green 2xPCR master mix (Peqlab) in an Eppendorf Realplex 2 Mastercycler according to manufacturer's instructions. The following PCR protocol was used for amplification:

1. Initial denaturation for 5 minutes at 95^{o}C
2. Denaturation at 95^{o}C for 10 seconds
3. Annealing at 58^{o}C for 20 seconds
4. Extension at 72^{o}C for 30 seconds

x40

Melting curve:
5. 95^{o}C for 15 seconds
6. 60^{o}C for 20 minutes
7. 95^{o}C for 15 seconds

Primers used for RT-qPCR:

Name	Primer sequence
LAP2α forward	GTGGGAACAACCAGGAAGCTATATGA
LAP2α reverse	TGAGTGCCTGCTGTGCATCACTA
Wildtype Lamin A/C forward	CTGCCGGCCATGGAGAC
Wildtype Lamin A/C reverse	GCTGACCACCTCTTCAGACT
mEos3.2 Lamin A/C forward	CATGCTGTTGCTCATTCTGGA
mEos3.2 Lamin A/C reverse	ACAAGTCCCCCTCCTTCTTGG
GAPDH forward	TGTGAACGGATTTGGCCGTA
GAPDH reverse	ACTGTGCCGTTGAATTTGCC

2.2.7 Live Cell Imaging

Transfection of cells

All the live cell imaging experiments were performed using transfected HeLa cells. For this purpose, HeLa cells were plated on 35mm 60µ-Glass Bottom Dishes (Ibidi) to ~20-25 percent confluency and incubated overnight. In order to transfect the cells, a mixture containing 100µl of Nanofectin diluent (GE Healthcare, PAA) and 10µl of Nanofectin was added to another mixture consisting of 100µl of Nanofectin diluent and 0.5µg of the plasmid containing the appropriate GFP-tagged construct. The final mixture was incubated for 25 minutes at room temperature and added dropwise to the cells. The medium on the cells was exchanged 3 to 4 hours post-transfection to Phenol red-free high-glucose DMEM supplemented with 20% FCS, 0.85mM ascorbic acid, 0.2µM L-Glutamine, 100U/ml penicillin and 100µg/ml streptomycin.

Constructs used for transfection

Four different plasmids were used to transfect LAP2α wildtype and knockout HeLa cells in order to perform the live cell imaging experiments. These plasmids contained an EGFP-tag fused to: a) pre-lamin A, b) mature lamin A, c) pre-lamin A ΔK32 and d) mature lamin A ΔK32. All vectors include a CMV promoter site, an SV40 terminator and a kanamycin resistance gene (Fig. 7).

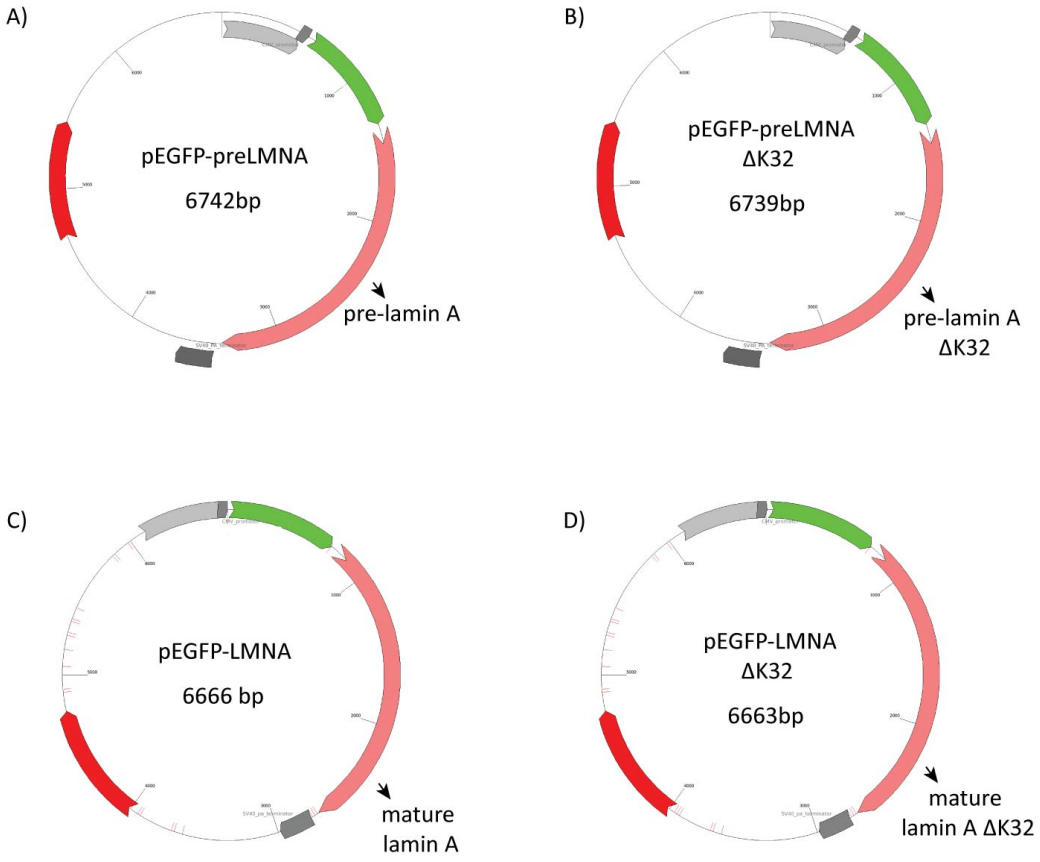

Figure 7. Vectors used for transfection. Vectors containing EGFP-tagged lamin constructs were ectopically expressed in HeLa cells using Nanofectin. CMV promoter site indicated in light grey, SV40 terminator indicated in dark grey, kanamycin resistance gene indicated in red.

Live cell imaging set up

Live cell imaging was performed using the same set up for two clusters of experiments. Cells transfected with different GFP-tagged constructs were imaged either 24 hours ('steady-state') or 4-5 hours ('emerging') post-transfection. The samples were imaged on an inverse spinning disk microscope using a 63x objective (Plan-Apochromat 63x/1.4 Oil DIC) and an EM-CCD camera under controlled environmental conditions of 37^{o}C and 5% CO_2. All the samples were imaged for 14-15 hours with 20-minute intervals, acquiring Z-sections of every field using the same excitation strength and exposure time.

Processing of live cell imaging data

Images were processed and evaluated using FIJI. First, all time-lapse images were smoothed by 1-pixel radius Gaussian Blur filter, appropriate time points were selected and further processed to create short movies and the images presented in the results section. The data were evaluated by drawing a 3 pixel wide bar across the nuclei of selected cells and creating plot profiles for each cell. A list of intensity values was created and the nucleoplasmic to peripheral lamin ratio was calculated. GFP-tagged lamin intensity at the periphery of the nucleus was determined as the average of two peak measurements, one from each end of the drawn line, and the nucleoplasmic intensity as the average of 30 measurements spanning the center of the drawn line. Cells displaying abnormal levels of overexpressed proteins as well as cells that could not be monitored throughout the experimental time course (240 minutes starting from time point 0) were discarded from the evaluation.

2.2.8 Single Cell High Throughput Imaging

Sample preparation

Cells expressing m3.2Eos-tagged endogenous lamin A/C were fixed and prepared for single cell high throughput analysis according to the Immunofluorescence protocol described in chapter 2.2.3. For these experiments, however, no antibody staining was used on the samples.

Imaging set up

The samples were imaged on an inverse spinning disk microscope using a 63x objective (Plan-Apochromat 63x/1.4 Oil DIC) and an EM-CCD camera. The laser excitation strength and exposure time were kept constant for all samples. To semi automate the data acquisition process, a Python script, written by Christian Knapp, was used. Using this plug-in, a raster was created based on three manually selected fields, defining the cover slip edges. For each sample, the raster consisted of at least 400 fields of vision, which were subsequently scanned using the appropriate lasers.

Processing and Evaluation of imaging data

Images were imported into FIJI and evaluated using a Python plug-in written by Christian Knapp. First, the cell cycle stage of each cell was determined based on the DAPI intensity and a cell cycle profile was created. For each cell that was detected in the scanned fields, the outline of the nucleus was determined based on the lamina staining and the nuclei were divided in two circular sections. The

peripheral lamin A/C value was determined as the mean value of the pixels included in the outer section (lamina) and the value of nucleoplasmic lamin A/C was set as the mean of the inner section. The nucleoplasmic/peripheral lamin A/C ratio of the cells was calculated and plotted against the cell cycle stage.

2.2.9 Biochemical Extractions

To evaluate the extractability of lamin A/C, cells were cultured overnight on 10cm dishes. The next day, cells were washed twice with PBS, scraped in 1ml of Extraction Buffer (see Materials), collected in 15ml falcons and incubated on ice for 10 minutes. Following the incubation, 200µl of each sample were transferred to Eppendorf tubes labeled as total lysate. The remaining sample was spun for 10 minutes at 4000rpm at 4^{o}C in a Heraeus table top centrifuge, 200µl of the supernatant were transferred to Eppendorf tubes labeled as soluble fraction. The pellet was resuspended in 800µl of Extraction Buffer and 200µl were transferred to Eppendorf tubes labeled as insoluble fraction. In each tube containing the 200µl fractions of the samples, 100µl of 3x Sample Buffer was added, the samples were incubated for 5 minutes at 95^{o}C. Protein levels in the different fractions of the samples were evaluated by Immunoblotting.

3. Results

3.1 Origin of nucleoplasmic A-type lamins

Although the presence of a nucleoplasmic fraction of lamins with distinct properties and functions from those of the nuclear lamina has been observed early on[61], the origin of intranuclear lamins still remains unclear. One potential pathway explaining the formation of the nucleoplasmic pool of lamins is based on a cell-cycle dependent mechanism, where a fraction of the phosphorylated disassembled lamins residing within the nucleoplasm in early G1 phase following mitotic cell division is prevented from assembling into the lamina and remains in a more soluble state throughout the cell cycle[57]. To study this putative origin of nucleoplasmic lamins, we decided to track the dynamics of lamin A in post-mitotic cells throughout G1 phase. For this purpose, we transiently expressed EGFP-pre-lamin A in HeLa cells and used long-term live cell imaging to track the GFP-tagged protein in mitotic and early stage (G1 phase) post-mitotic nuclei. Cells were imaged 24 hours post-transfection (Fig. 8A, left), and, thus at the beginning of the time course the ectopically expressed precursor of lamin A was already processed into mature lamin A. Monitoring the dynamics of EGFP-lamin A in newly forming nuclei, and in line with what has been reported so far[72-73, 98], we were able to detect the formation of a prominent nucleoplasmic pool of lamins in early G1 (time point 20'). As the cell cycle progressed in G1, we observed the majority of EGFP-lamin A gradually assembling into the lamina, while a fraction was not recruited to the nuclear periphery and remained nucleoplasmic. Following our observations, we could conclude that, at least partially, nucleoplasmic A-type lamins indeed originate from the preceding mitosis.

It is reasonable to assume that newly synthesized pre-lamin A might also participate in the generation of the nucleoplasmic pool of lamins in post-mitotic nuclei. To further investigate this scenario, we utilized the same experimental set-up to transiently express EGFP-pre-lamin A in HeLa cells. However, in these experiments, cells were imaged 4-5 hours post transfection (Fig. 8A, right), in order to tack solely newly synthesized, unprocessed pre-lamin A. We selected exclusively for cells that showed no sign of fluorescence before mitosis, and only started expressing GFP-pre-lamin A after cell division (time point 0'). In this case, we observed that the newly emerging pre-lamin A localized exclusively to the nuclear periphery of the newly formed nuclei before a fraction of it was released into the nucleoplasm, most likely paralleling its maturation and removal of the C-terminal farnesylation. This shows that, indeed, newly synthesized pre-lamin A constitutes an additional source of nucleoplasmic A-type lamins, without the need to go through a mitotic cell division.

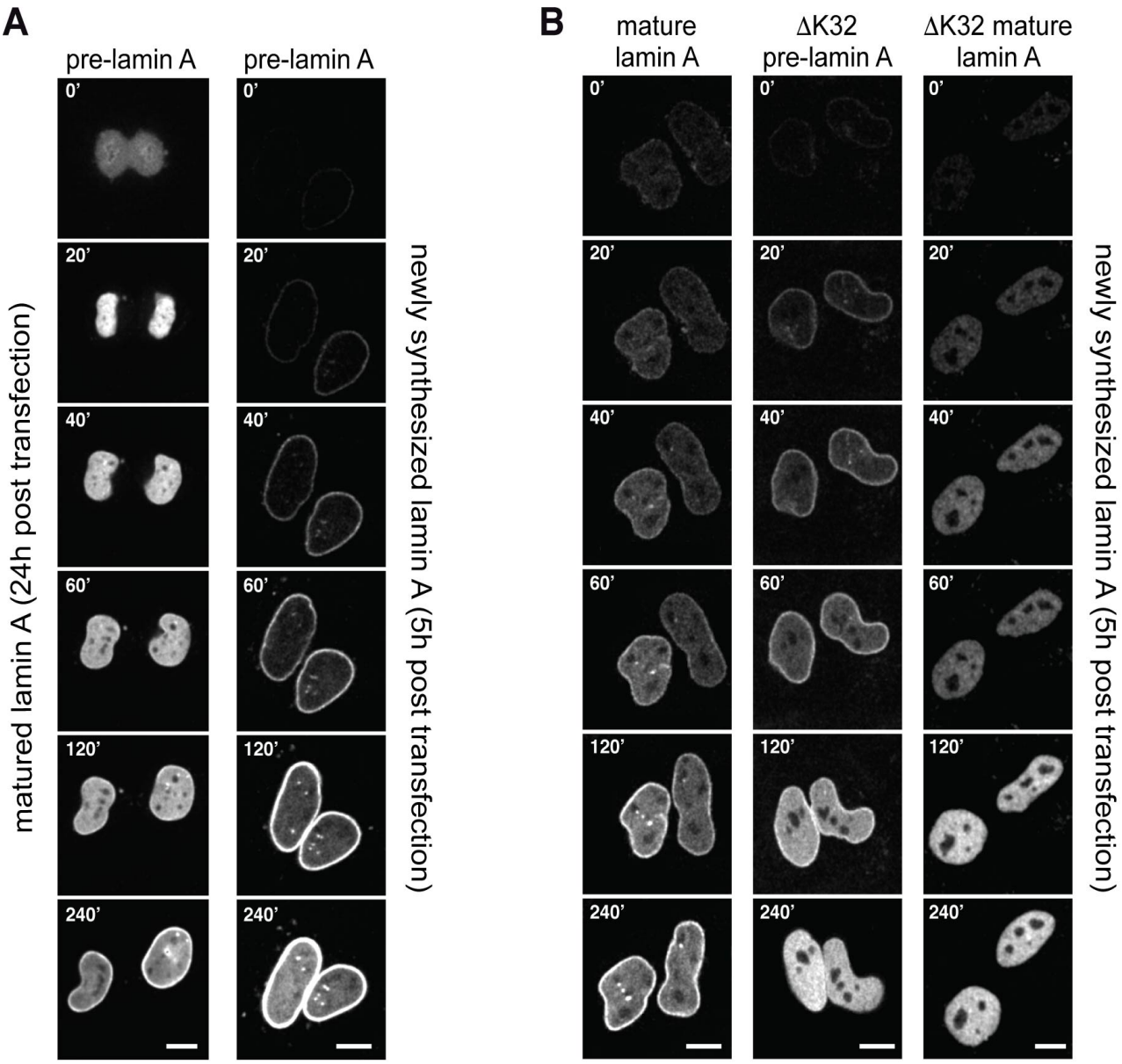

Figure 8. Origin of the nucleoplasmic lamin A pool in post-mitotic nuclei and lamin A processing dynamics. (A) HeLa cells were transiently transfected with EGFP-pre-lamin A and analyzed by live-cell imaging 24 hours (left) or 5 hours (right) post transfection. **(B)** EGFP-tagged constructs were transiently expressed in HeLa cells as indicated and monitored by live imaging 5 hours post transfection. Numbers indicate minutes. Scale bar: 10μm.

3.2 Dynamics of lamin A post-translational processing

Pre-lamin A undergoes a series of processing steps, initiated by the C-terminal farnesylation of the protein. The isoprenylation reaction is followed by a proteolytic cleavage, methylation and an additional cleavage of the C-terminus, ultimately yielding mature lamin A. It is believed that, following its nuclear transport and farnesylation, pre-lamin A is targeted to the nuclear membrane, where the remaining post-translational modifications take place. In our experiments, we could indeed observe the initial recruitment of newly synthesized, ectopically expressed pre-lamin A to the nuclear membrane (as seen in Fig. 8A, right) prior to its release into the nucleoplasm, which indicates that processing of pre-lamin A occurs at the nuclear periphery. To further investigate the dynamics of lamin-A processing, we transfected HeLa cells with EGFP-mature lamin A, which is expressed as fully processed lamin A, therefore bypassing the post-translational modification process. In contrast to newly expressed pre-lamin A, mature lamin A 'emerges' within the nucleoplasm and is detected at the nuclear periphery approximately 40 minutes later (Fig. 8B, left). The distinct dynamics of newly synthesized mature lamin A compared to pre-lamin A support the hypothesis that addition of the farnesyl-group quickly targets pre-lamin A to the nuclear membrane, followed by its processing and release of a subfraction into the nucleoplasm.

Moreover, we ectopically expressed constructs containing the precursor and the mature form of lamin A-ΔK32 in HeLa cells. Lamin A-ΔK32 is a variant of lamin A harboring a deletion of the lysine in position 32, identified in patients with specific striated muscle laminopathies (Emery–Dreifuss muscular dystrophy and LMNA-related congenital muscular dystrophy)[99]. As a result of this mutation in the N-terminal domain, lamin A-ΔK32 displays an assembly defect and is, therefore, unable to integrate into the lamina. Nevertheless, we observed that newly synthesized EGFP-pre-lamin A-ΔK32 initially localized to the nuclear periphery and gradually translocated to the nuclear interior during G1, until it was detectable only in the nucleoplasm (Fig. 8B, middle). On the other hand, ectopic mature lamin A-ΔK32 was not detected at the nuclear membrane at any time point during the imaging time course (Fig. 8B, right). Based on our observations from these experiments, we can deduce that the farnesylation of pre-lamin A is sufficient for its fast recruitment to the nuclear periphery, followed by further post-translational processing and removal of the farnesyl group. Unassembled or assembly-deficient (ΔK32) lamin A is then released into the nucleoplasm. Constructs lacking the farnesylation site, on the contrary, are recruited to the periphery during filament assembly in G1 phase or – in case of assembly-deficient lamins – remain nucleoplasmic.

3.3 Regulation of nucleoplasmic lamin A by LAP2α

It was demonstrated by Naetar et al[59] that dermal fibroblasts isolated from LAP2α-deficient mice exhibit significantly reduced levels of intranuclear lamin A/C, showing that LAP2α regulates the nucleoplasmic pool of A-type lamins. Since the reduction of nucleoplasmic lamins in LAP2α-deficient mice was most prominent in G1 cells, we reasoned that, in LAP2α knockout cells, the dynamics of lamin A during post-mitotic lamina assembly might be altered compared to control cells. In particular, we speculated that the fraction of lamins remaining in the nucleoplasm after lamina assembly in G1 might be altered and/or reduced in the absence of LAP2α.

3.3.1 Influence of LAP2α on nucleoplasmic lamin A originating from the preceding mitosis

As described in chapter 3.1, we identified two sources of nucleoplasmic lamin A: mature lamin A remaining in the nucleoplasm after mitosis and newly synthesized lamin A, being released into the nucleoplasm after its initial farnesyl-dependent recruitment to the nuclear periphery and processing. In order to investigate the distribution pattern of lamin A originating from the preceding mitosis, we ectopically expressed EGFP-pre-lamin A in LAP2α wildtype and knockout HeLa cells (previously created in the lab using CRISPR/Cas9) and tracked the dynamics of fully processed EGFP-mature lamin A 24 hours post transfection in post-mitotic nuclei (Fig. 9A). Surprisingly, we did not observe lower levels of intranuclear lamin A in LAP2α-deficient cells compared to wildtype cells (Fig. 9A, last row, time point 240'). To verify our observation, we proceeded to quantify the intensity of EGFP-lamin A. The distribution of lamin A across the nucleus over a 4-hour time course is represented by the ratio of nucleoplasmic to peripheral mean lamin A intensity (Fig. 9C). During late telophase (time point 0'), lamin A is dispersed throughout the mitotic nucleus, therefore the nucleoplasmic/peripheral lamin A ratio was set as 1. We observed that, during the first hour, there is little change in the ratio, meaning that the majority of lamin A remains nucleoplasmic. Subsequently, lamin A begins to assemble into the peripheral lamina, and this is reflected as a decrease in the nucleoplasmic/peripheral lamin A ratio. Comparing the LAP2α wildtype and knockout lamin A-distribution curves we found that, overall, absence of LAP2α does not have a significant effect on the dynamics of mature lamin A, while the cells progress through G1 phase.

3.3.2 Effect of LAP2α on nucleoplasmic lamin A originating from newly synthesized lamins

Considering the results of our live-cell imaging experiments, which revealed that LAP2α does not influence the levels of mature lamin A reassembling into the lamina after mitosis, we hypothesized that the previously described reduction of nucleoplasmic lamins could be attributed to the altered distribution of newly synthesized lamin A in the absence of LAP2α. Therefore, we monitored the newly 'emerging' lamin A in LAP2α ($^{+}/^{+}$) and LAP2α ($^{-}/^{-}$) HeLa cells transiently expressing EGFP-pre-lamin A 5 hours post transfection (Fig. 9B). Surprisingly, once again, there was no reduction of nucleoplasmic lamin A levels. Even after several hours of imaging, when the overexpressed pre-lamin A is fully processed and the nucleoplasmic pool of lamin A has already formed in late G1 (Fig. 9B, last row, time point 240'), levels of intranuclear lamin A remained similar in LAP2α wildtype and knockout cells. Furthermore, the nucleoplasmic to peripheral ratio of EGFP-lamin A did not display a significant difference in the distribution of newly synthesized lamin A in the absence of LAP2α (Fig. 9D).

3.3.3 Distribution of different newly synthesized lamin A constructs is not influenced by LAP2α

Finally, we investigated whether lack of LAP2α would alter the distribution of other lamin A constructs. We, therefore, ectopically expressed EGFP-mature lamin A, EGFP-pre-lamin A-ΔK32 and EGFP-mature lamin A-ΔK32 in LAP2α knockout HeLa cells and monitored the distribution of newly synthesized lamin A constructs. We compared the dynamics of the constructs in LAP2α ($^{-}/^{-}$) cells to the data previously obtained for wildtype control cells and did not detect any changes throughout G1 (Fig. 10).

Interestingly, in some cells, overexpression of pre-lamin A-ΔK32 resulted in formation of misshaped nuclei. While tracking the distribution of the EGFP-tagged lamin construct we noticed that the number of deformed nuclei expressing ΔK32 was higher in wildtype cells, when compared to LAP2α knockout. Specifically, 66% of nuclei displayed abnormal morphology in wildtype cells, while in LAP2α knockout cells the percentage of misshaped nuclei was only 31%. Representative images of distorted and normally shaped nuclei are depicted in Figure 11. It is unclear whether this phenomenon is somehow related to altered mechanical properties of the lamina in the absence of LAP2α. We did not look further into this issue; however, more experiments could shed light on this interesting observation in the future.

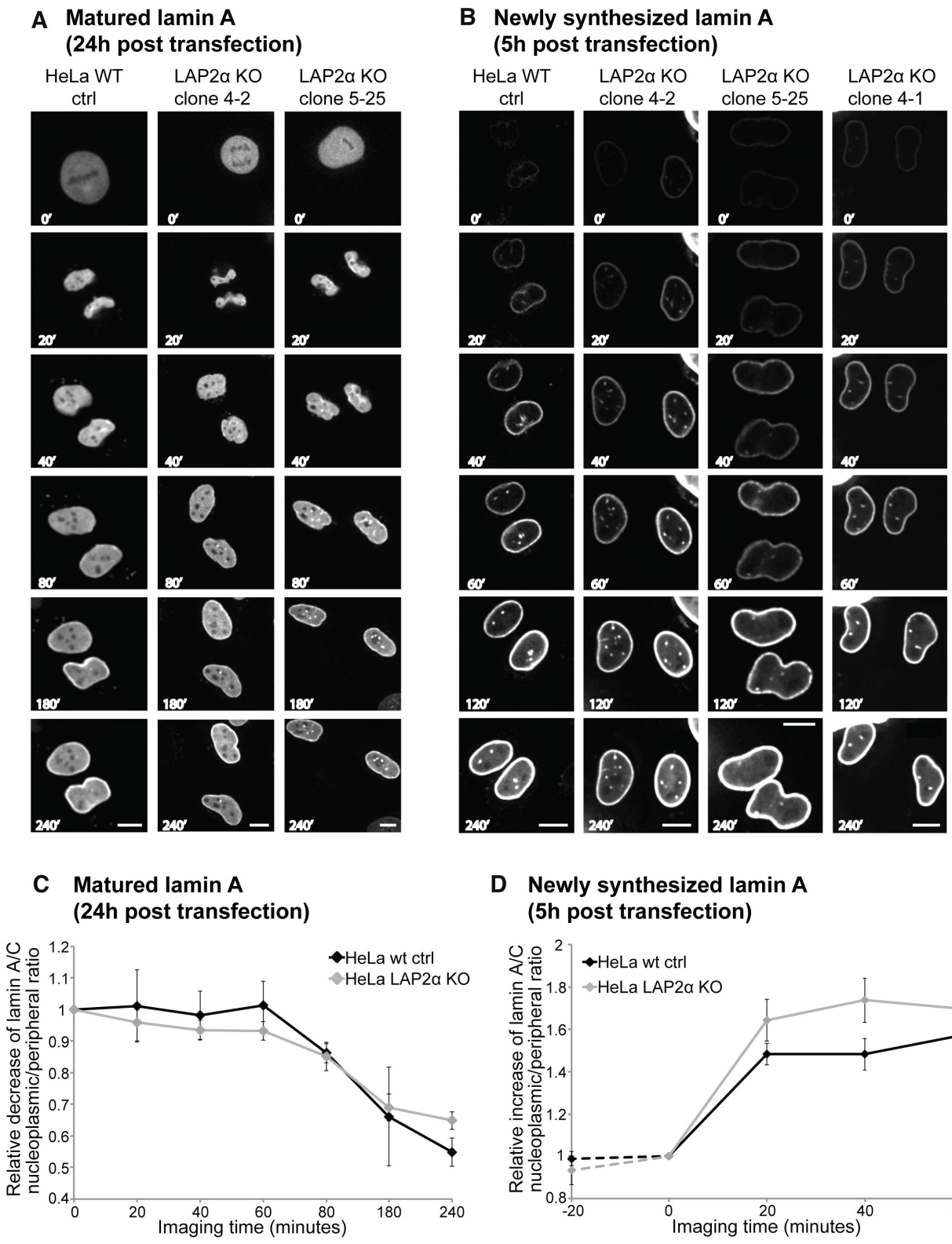

Figure 9. Absence of LAP2α does not alter the distribution of lamin A during post-mitotic nuclear lamina assembly or during pre-lamin A synthesis and processing. (A-B) LAP2α

($^{+}/^{+}$) and ($^{-}/^{-}$) HeLa cells were transiently transfected with EGFP-pre-lamin A and analyzed by live-cell imaging either 24 hours **(A)** or 5 hours **(B)** post transfection. Numbers indicate minutes. Scale bar: 10μm. **(C-D)** Nucleoplasmic to peripheral mean signal intensity of EGFP-lamin A was calculated and plotted versus imaging time normalized to the ratio in mitosis/early G1 (time point 0'), creating a lamin A distribution pattern in post-mitotic nuclei of LAP2α wildtype (black line) and knockout (grey line) cells. **(C)** Distribution of fully matured lamin A after mitotic cell division. Measurements obtained from cells shown in 9A, n_{WT}=2, n_{KO}=4. **(D)** Newly synthesized lamin A distribution. Cells originating from three LAP2α knockout clones were analyzed and the measurements were combined. n_{WT}=18, n_{KO}=23. We defined as time point 0' the moment preceding a significant increase of nucleoplasmic lamin A in each cell. Subsequently, we calculated the nucleoplasmic to peripheral ratio of EGFP-lamin A for the following 60 minutes. Dashed lines indicate measurements performed in smaller number of cells (n_{WT}=6, n_{KO}=6), demonstrating that nucleoplasmic to peripheral ratio prior to the initial release of lamin A into the nucleoplasm (time point 0') is maintained at steady levels.

Taken together, our live-cell imaging data indicate that lack of LAP2α does not alter the dynamics of mature lamin A reassembly or of the incorporation of newly synthesized lamin A into the lamina. These findings directly contradict previous studies, where it was suggested that LAP2α regulates the levels of nucleoplasmic A-type lamins[59, 81]. One possibility is that these unexpected observations are due to overexpression of EGFP-tagged lamin constructs. While ectopic expression of proteins fused to fluorescent markers is a widely used method for microscopic investigation of protein properties, it has raised concerns that it might not reflect the behavior of the endogenous protein. In our experiments, we noticed that, in some cells, ectopically expressed EGFP-lamin A constructs formed aggregates within the nucleus and that high expression of the constructs usually resulted in cell death. It is therefore conceivable that the properties of ectopically expressed lamin A, fused with a large fluorescent molecule such as EGFP, might differ from those of the endogenous lamin A.

We decided to further investigate the role of LAP2α in the regulation of nucleoplasmic A-type lamins using endogenously tagged lamin A/C. Inserting a fluorescent tag into the desired location (LMNA gene) provides an excellent system for monitoring protein localization while maintaining the innate regulation and gene expression pattern of this particular protein.

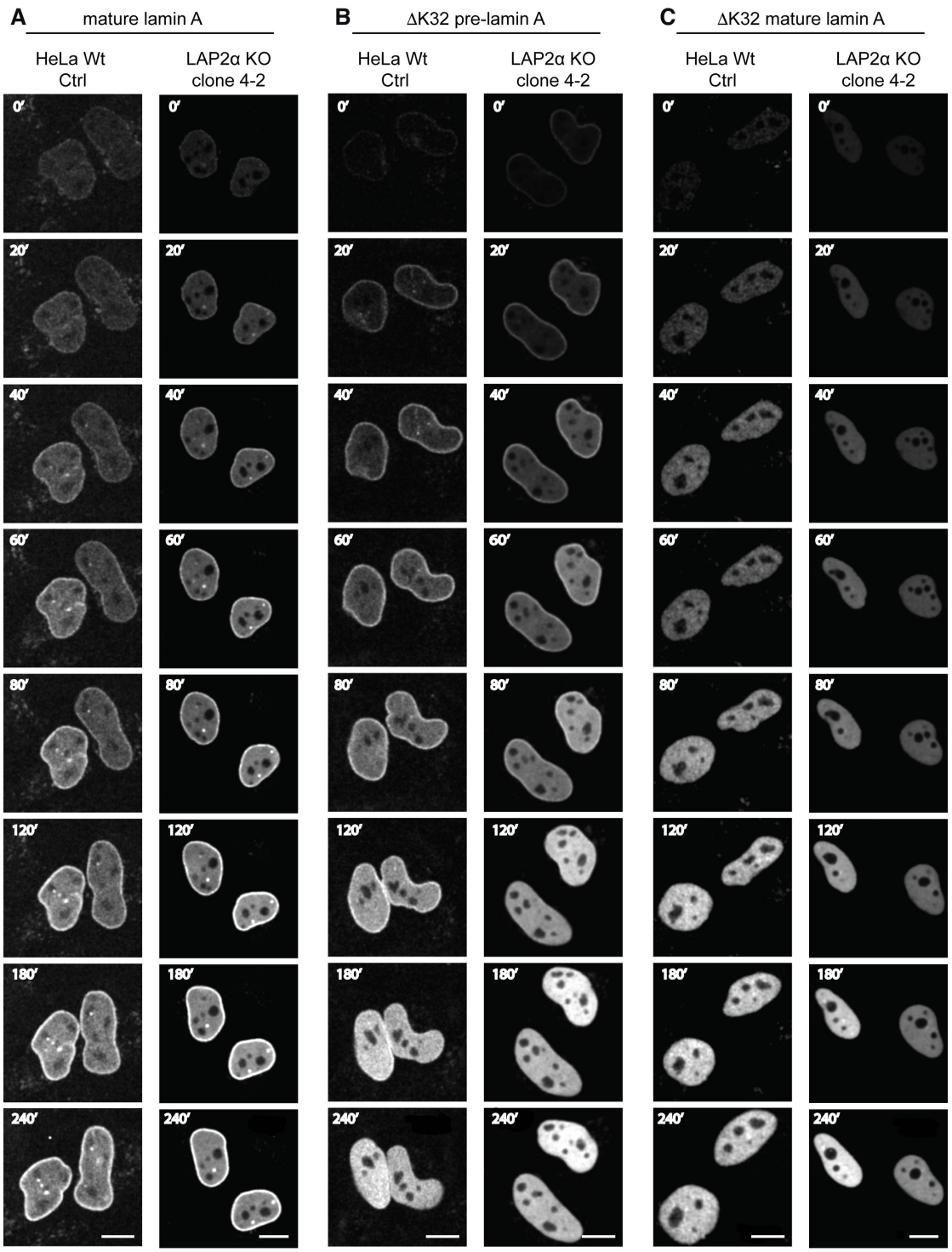

Figure 10. Dynamics of newly produced lamin A constructs is not affected by LAP2α. Side-by-side comparison of LAP2α ($^{+}/^{+}$) and ($^{-}/^{-}$) HeLa cells transiently transfected with **(A)** EGFP-mature lamin A, **(B)** EGFP-pre-lamin A-ΔK32 and **(C)** EGFP-mature lamin A-ΔK32 and analyzed by live cell imaging 5 hours post transfection. Numbers indicate minutes. Scale bar: 10μm.

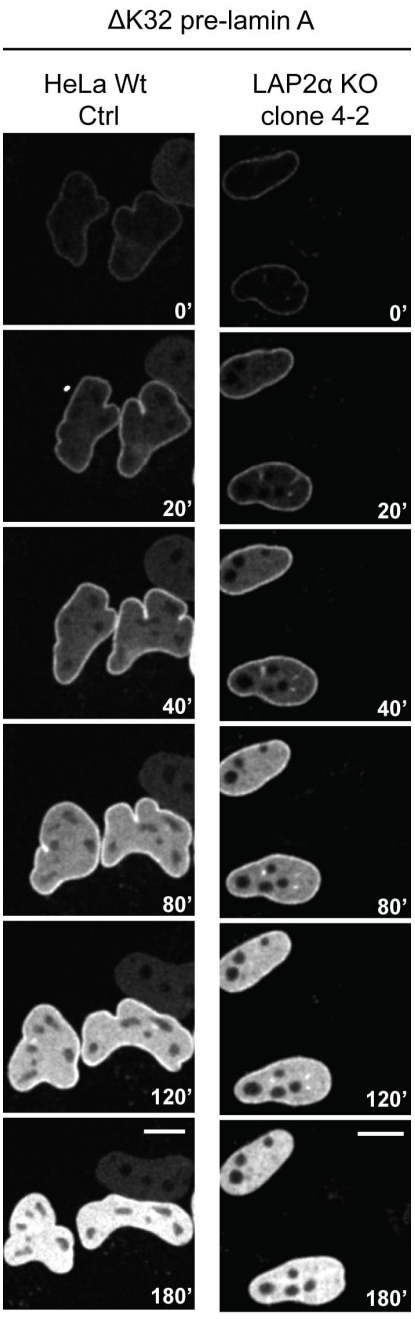

Figure 11. Altered nuclear morphology in EGFP-pre-lamin A-ΔK32 expressing cells differs in wildtype versus LAP2α knockout cells. Wildtype and LAP2α KO HeLa cells were transiently transfected with EGFP-pre-lamin A-ΔK32 and analyzed by live cell imaging 5 hours post transfection. Images indicate representative examples of deformed and normal nuclei mentioned in the text. Numbers indicate minutes. Scale bar: 10µm

3.4 Studying the effect of LAP2α on endogenous nucleoplasmic A-type lamins

Until recently, most microscopic studies depended on transient or constitutive protein overexpression. Ectopic expression of proteins has been held responsible for introducing several artifacts, such as protein mislocalization and aggregation, as well as unbalanced gene dosage[100]. Since manipulation of the mammalian genome has become increasingly easy, inexpensive and effective with the discovery of CRISPR/Cas9-mediated gene editing[101], generation of gene-edited cell lines, where a fluorescent marker is integrated at a specific locus, has become the preferred method for investigating protein activities. Modification of endogenous loci allows analysis of natively expressed and regulated proteins and, at the same time, eliminates the overexpression-induced artifacts. Therefore, we decided to study the regulation of nucleoplasmic A-type lamins by LAP2α using genome-edited cells, expressing endogenously tagged lamin A/C. Generation of the cell lines described below was performed by Nana Naetar.

3.4.1 Generation of fluorescently tagged-LMNA wildtype and LAP2α knockout mouse dermal fibroblasts

Generation of cell lines carrying a fluorescent tag on the LMNA gene was achieved using the CRISPR/Cas9 technology for gene editing[102]. In brief, Cas9 (CRISPR-associated protein 9) is a DNA endonuclease creating double strand breaks (DSBs) at specific sites, directed by a short guide RNA (sgRNA). The sgRNA is complementary to the site targeted for DSB, and consists of a 20bp sequence followed by a protospacer-adjacent motif (PAM), which facilitates target site-recognition by the endonuclease. The DSBs induced by Cas9 can be repaired by two cell-intrinsic mechanisms, nonhomologous end joining (NHEJ) and homology-directed repair (HDR)[103]. NHEJ repair induces different sized deletions or insertions, causing a frame shift of the open reading frame and disruption of protein production due to pre-mature stop-codons. On the other hand, precise modification of the target site can be achieved by HDR-mediated repair, using a 'donor template' containing the desired sequence modifications flanked by sequences homolog to the targeted locus.

Targeting the desired locus was achieved by designing a LMNA-specific sgRNA (sgRNA1) directing a Cas9-mediated double strand break in exon 1 (Fig. 12). A targeting vector containing the fluorescent marker gene provides the 'donor template', which is inserted at the site of the DSB by HDR. In this way, a knock-in allele is generated, where lamin A (and lamin C) is fused to a fluorescent protein, mEos3.2, at its N-terminus. mEos3.2 is a member of the green fluorescent protein family, which can be

irreversibly photoconverted from green to red emission upon photoactivation by ultraviolet light (~400nm)[97, 104].

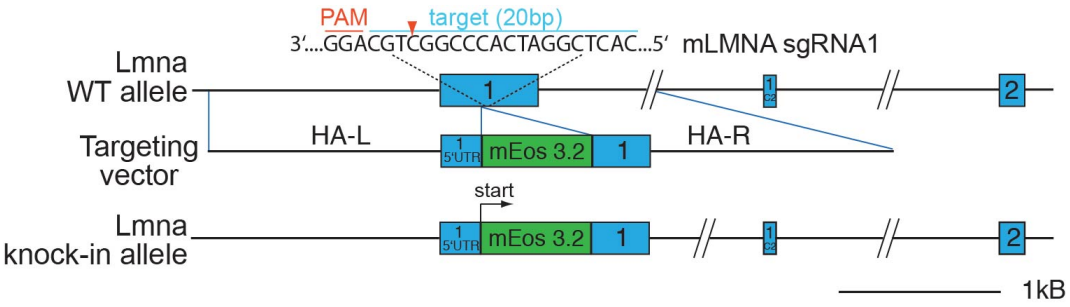

Figure 12. Schematic representation of CRISPR/Cas9-mediated generation of mEos3.2-LMNA mouse fibroblasts. Schematic view of LMNA locus targeted by Cas9 for homology-directed repair using the targeting vector as template, leading to the formation of a fluorescently tagged LMNA knock-in allele. Red arrow indicates the expected Cas9 cut site. (HA-L: Homology Arm-Left; HA-R: Homology Arm-Right, PAM: Protospacer adjacent motif).

LAP2α wildtype and knockout mouse dermal fibroblasts were transfected with all the necessary components for CRISPR/Cas9-mediated gene editing (sgRNA1, Cas9 and targeting vector). Single cell clones expressing the fluorescent marker were obtained by fluorescence-activated cell sorting (FACS) and evaluated by PCR for the presence of the knock-in allele, as well as for the proper 3-prime and 5-prime integration of the construct in the LMNA locus (representative PCR results are shown in Fig. 13B, C). Clones displaying proper integration of mEos3.2 were then processed for Western blot analysis in order to verify the expression of mEos3.2-lamin A/C and to assess protein levels. Finally, clone 21, derived from wildtype mouse dermal fibroblasts (hereafter named WT#21), was selected for further experimental procedures, because expression levels of endogenous lamin A/C, lamin B1 and LAP2α and β were similar to those of the control cell lines (MDF Wt and KO). Wildtype clone 5 and LAP2α knockout clone 17 are expressing only mEos3.2 lamin A/C and no endogenous allele, and were thus used in further experiments (Fig. 13D).

In order to study the influence of LAP2α on nucleoplasmic A-type lamins in the most effective way, mEos3.2-LMNA mouse fibroblasts from clone WT#21 were used for the generation of isogenic LAP2α knockout clones. This was favorable over using independently created Eos-tagged knockout MDF clones that displayed varying amounts of endogenous lamin A and Eos3.2-lamin A expression (Fig13D and data

not shown). CRISPR/Cas9-mediated depletion of LAP2α in WT#21 cells was achieved by targeting the LAP2α-specific exon of the *Tmpo* gene (exon 4), using two different sgRNAs, sgRNA1 and sgRNA3 (Fig. 13E).

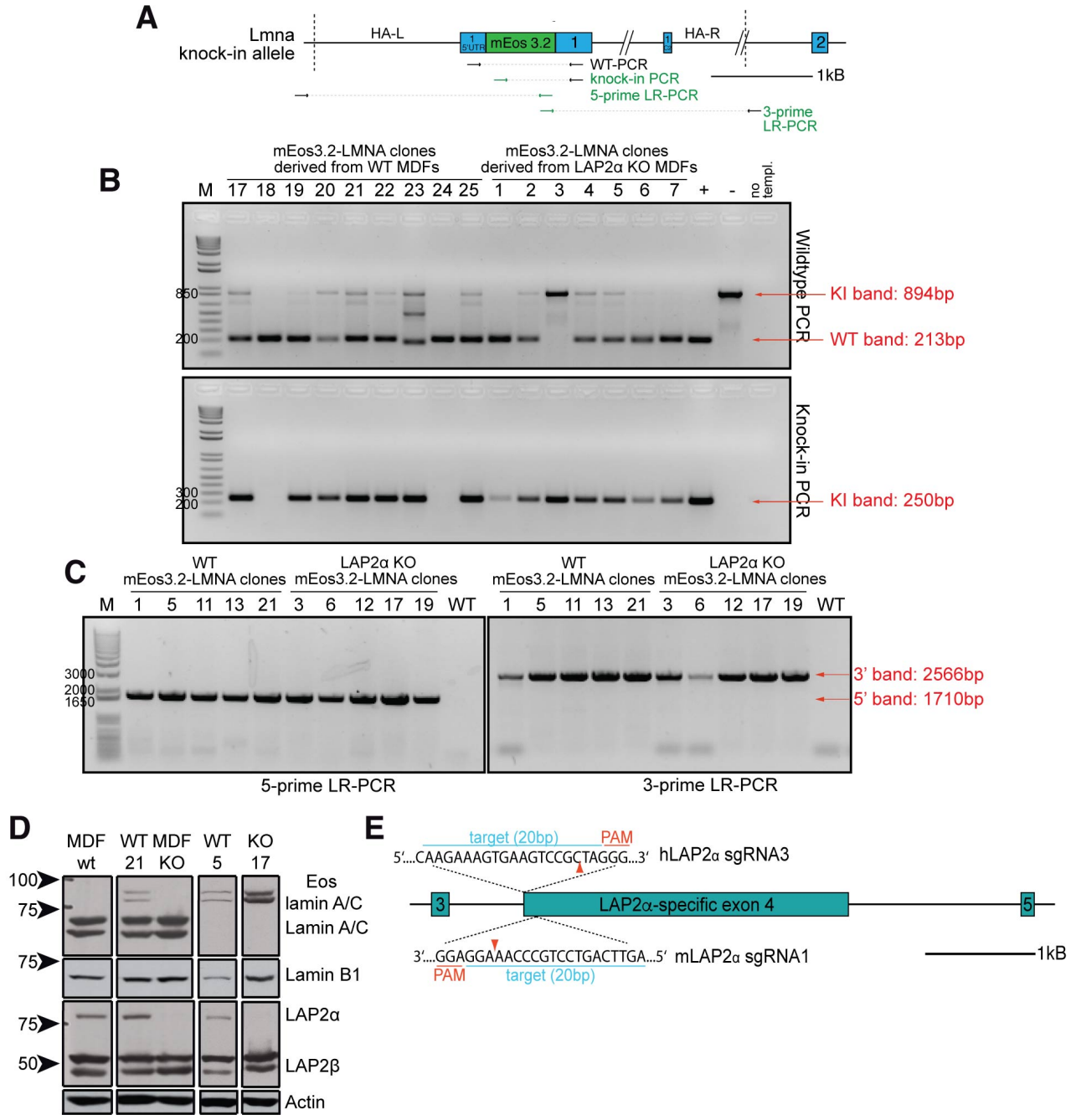

Figure 13. Generation of mEos3.2-LMNA knock-in LAP2α wildtype and knockout single cell clones. (A) Schematic view of the targeted LMNA locus after integration of mEos3.2. Arrows indicate the primers used for genotyping and long-range (LR) PCRs, green arrows indicate primers specific for knock-in allele. (HA-L: Homology Arm-Left; HA-R: Homology Arm-Right).

Genomic DNA was isolated from LAP2α wildtype (WT) and knockout (KO) mouse dermal fibroblast (MDF) clones and analyzed by PCR, using the primers indicated in (A), to determine the clonal genotype **(B)** and to test for proper construct integration **(C)**. **(D)** Western blot analysis of relevant LAP2α WT and KO mEos3.2-LMNA clones using antibodies to the indicated antigens. **(E)** Schematic view of the LAP2α locus targeted by CRISPR/Cas9. The sequences of both short-guide RNAs used (sgRNA1, sgRNA3) are indicated. Red arrow indicates the expected Cas9 cut site. (PAM: Protospacer adjacent motif).

3.4.2 Characterization of mEos3.2-LMNA mouse dermal fibroblasts

Following the establishment of mEos3.2-LMNA wildtype (WT#21) and isogenic LAP2α knockout mouse dermal fibroblasts, we proceeded to characterize the CRISPR-Cas9 generated clones. First, we processed cells derived from sgRNA1- (Sg1) and sgRNA3- (Sg3) treated clones in order to test for LAP2α expression. As depicted in Fig. 14A (middle panel), in clones Sg1-1, Sg1-2, Sg3-7 and Sg3-8 LAP2α has been depleted. Next, we tested the expression of mEos-tagged and untagged lamin A/C (Fig. 14A, upper panel). We observed similar expression levels of endogenous wildtype lamin A/C in the edited cell lines compared to control cell lines (MDF wt and KO) and similar levels of the tagged protein in all clones. Immunofluorescence microscopy revealed that nuclei from most mEos-LMNA cell lines displayed physiological morphology and verified the expression and correct localization of mEos3.2 lamin A/C, as well as the absence of LAP2α in knockout clones (Fig. 14B).

As mentioned previously, knockout of LAP2α was achieved using CRISPR/Cas9 to target the LAP2α-encoding *tmpo* locus for double strand break, which is repaired by NHEJ and results in random deletions or insertions at the target site. Therefore, due to faulty DNA repair, a frameshift is introduced which can lead to the production of mutated mRNAs containing premature stop codons. In mammalian cells, such mRNAs are usually degraded by a process called non-sense mediated mRNA decay (NMD), resulting in the depletion of both the mRNA and protein[105]. Some mRNAs containing premature stop codons can escape NMD and produce truncated proteins. However, incomplete, instable and nonfunctional proteins are usually degraded by proteases. Thus, in this case, even though the mRNA may be present, no protein is detected in the cells.

To find out whether nonsense-mediated decay of LAP2α mRNA is taking place in the CRISPR/Cas9-generated LAP2α knockout cells, we tested the level of LAP2α mRNA in wildtype and

knockout mEos3.2-LMNA clones using quantitative real-time PCR. As depicted in Fig. 14C, LAP2α mRNA is detected in all clones at different levels. Both wildtype clones (WT#21 and Sg3-2) display high levels of mRNA, while clone Sg1-4, which is characterized as a LAP2α heterozygote based on our Western blot analysis (Fig. 14A), has reduced levels of mRNA. Finally, in knockout clone Sg1-2, LAP2α mRNA is nearly depleted, whereas we detected significant levels of mRNA in the second knockout line (Sg3-8). Thus, nonsense-mediated decay seems to take place in some, but not all LAP2α knockout clones.

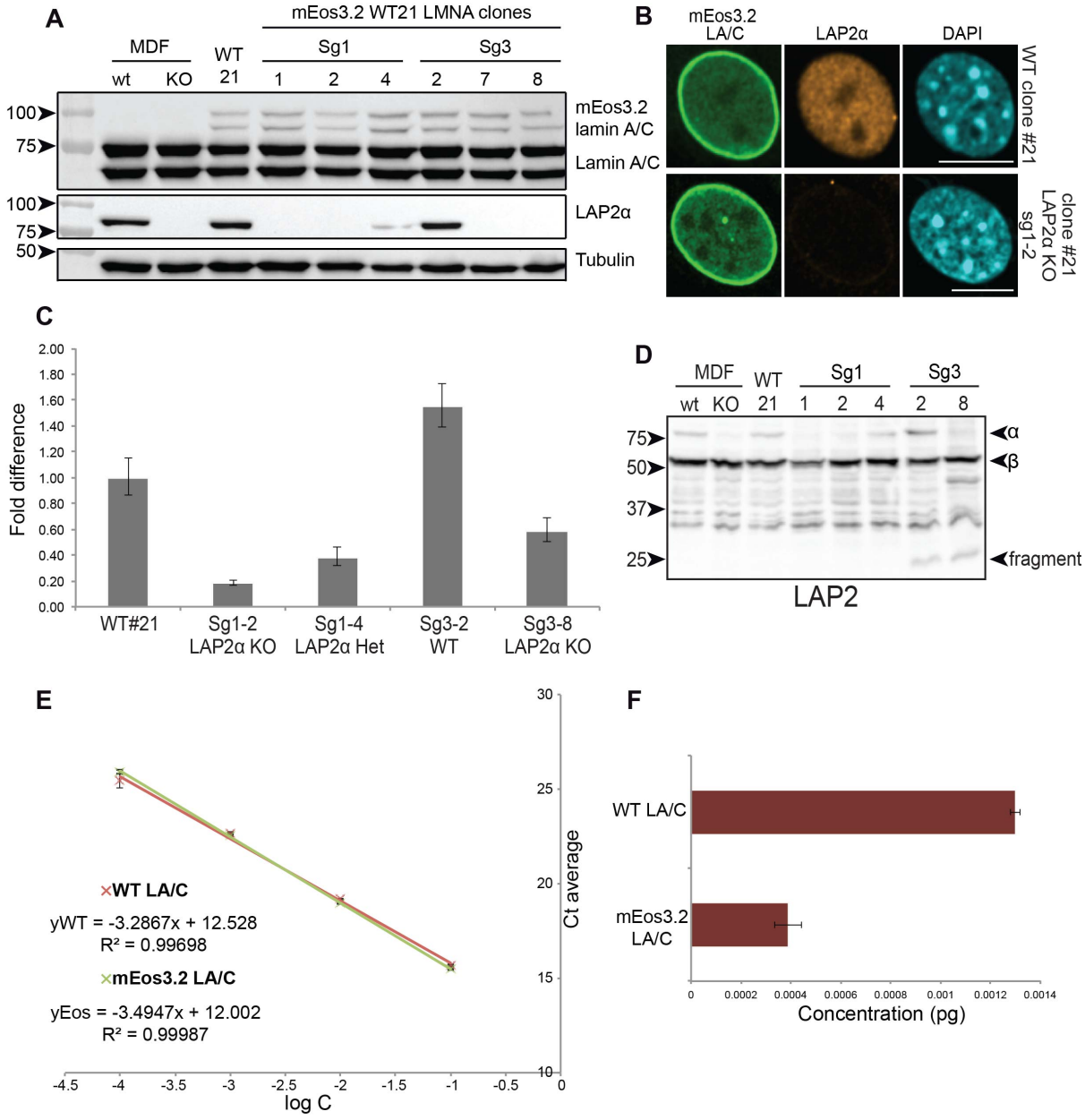

Figure 14. Characterization of mEos3.2-LMNA mouse fibroblasts. Isogenic mEos3.2-LMNA wildtype (WT) and LAP2α knockout (KO) clones were processed for **(A)** Western

blot analysis and **(B)** Immunofluorescence microscopy using antibodies against the indicated antigens. Scale bar: 10µm. **(C)** Isogenic clones were processed to determine LAP2α mRNA levels by qRT-PCR. **(D)** Isogenic clones were processed for Western blotting using an antibody against the LAP2 N-terminal common domain. **(E)** Standard curves for primer pairs detecting wildtype and mEos3.2 lamin A/C. (logC: decadic logarithm of DNA concentration). **(F)** DNA concentration of tagged and untagged lamin A/C in the WT#21 clone. **(C, E-F)** Graphs show average values ± standard error, n= 3.

Considering that LAP2α mRNA was present in some clones (e.g. sg3-8, Fig. 14C), where full length LAP2α protein was not detected by Western blot analysis (Fig. 14A), we proceeded to test whether a truncated form of the protein might escape protease-degradation and is present in the cells. We analyzed the clones by Western blot using an antibody against an epitope located in the LAP2 N-terminal common domain and, hence, detects all LAP2 isoforms. As seen in Fig. 14D, WT#21 and Sg1-treated clones have similar LAP2-isoform expression patterns that overlap with control mouse fibroblasts (MDF wt and KO), whereas in the Sg3-treated clones a LAP2 fragment (approximately 25KDa) was detected. This fragment most likely corresponds to the truncated protein variant encoded by the mutated LAP2α mRNA. Truncated mutant proteins can have dominant negative effects on cells and interfere with their characteristics. Although cells derived from Sg3 mEos-LMNA clones displayed normal viability and morphology, the presence of a LAP2α-fragment might influence our results. For this reason, when we used these cell lines in further experiments, we directly compared the wildtype (Sg3-2) to the LAP2α knockout (Sg3-8) clone.

To complete the characterization of the mEos-LMNA fibroblasts, we evaluated how many knock-in alleles are present in our cell lines. Genetic characterization of WT#21 cells by performing PCRs across the targeted locus, followed by sequencing and analysis, revealed that this immortalized cell line is tetraploid and harbors wildtype, as well as knock-in alleles (data not shown). To determine how many alleles produce tagged lamin A/C, we compared the amount of tagged and untagged lamin A/C transcripts in WT#21. We started by isolating mRNA from WT#21 cells and synthesizing cDNA, which we used as template for the PCR amplification of wildtype and mEos3.2 lamin A/C. We quantified the amplification products and created serial dilutions of known concentration, which served as templates for RT-qPCR using the same primers that detect wildtype and Eos lamin A/C. Using the measured samples, we created a standard curve plotting the Ct value against the concentration of DNA contained

in the sample (Fig. 14E). Using this standard curve, it was possible to calculate the absolute quantity of wildtype and mEos3.2 lamin A/C cDNA in cells derived from clone WT#21. We found that the cDNA concentration of untagged lamin A/C is 3.3 times more than Eos lamin A/C (Fig. 14F), indicating that the mRNA content of the cells is approximately ¾ wildtype and ¼ mEos-LMNA mRNA. Since all the cell lines originate from WT#21, our finding shows that all mEos3.2-LMNA wildtype and LAP2α knockout clones are tetraploid (confirming the genetic analysis) and only one allele carries the fluorescent tag.

3.4.3 Absence of LAP2α does not alter mEos3.2-lamin A/C nucleoplasmic/peripheral ratio

As discussed previously, experiments based on protein overexpression must be taken with caution, since the method has been shown to introduce many artifacts. Generation of the mEos3.2-LMNA cell lines provided us with the opportunity to study the influence of LAP2α on endogenously tagged nucleoplasmic lamin A/C.

We performed single cell high throughput analysis to investigate the distribution of mEos3.2 lamin A/C during different cell cycle stages. Isogenic wildtype and LAP2α knockout mouse fibroblasts were fixed, stained with DAPI to visualize DNA, and imaged. Based on the fluorescent intensity of DAPI, we estimated the DNA content of each cell and created a cell cycle profile (Fig. 15A)[106]. At the same time, we measured the peripheral and internal signal intensities of mEos-lamin A/C in every cell. Therefore, we were able to calculate the nucleoplasmic to peripheral lamin A/C ratio of LAP2α wildtype and knockout cells in G1 and S/G2 phase (Fig. 15B).

Based on results previously generated in the lab[59], we expected that loss of LAP2α would impact the distribution of endogenous lamin A/C across the nucleus. Surprisingly, however, our analysis revealed no differences between wildtype and knockout mouse fibroblasts (Fig. 15). These findings are consistent with our live-cell imaging data, suggesting that absence of LAP2α does not change the dynamics of lamin A/C, but they contradict former studies, which have revealed a significant reduction of nucleoplasmic lamin A/C in LAP2α-depleted cells[59, 81].

In order to avoid potential artifacts caused by fixation of the cells, Christian Knapp performed live-cell imaging of isogenic mEos3.2-*LMNA* LAP2α wildtype and knockout clones analyzing the distribution of tagged endogenous lamin A/C in the nucleus. In this analysis, single mitotic cells were tracked over time and the ratio of nucleoplasmic over peripheral mEos3.2 lamin A/C was calculated.

Once again, the results demonstrated no significant difference in post mitotic dynamics of lamin A/C in LAP2α wildtype and knockout cells (data not shown).

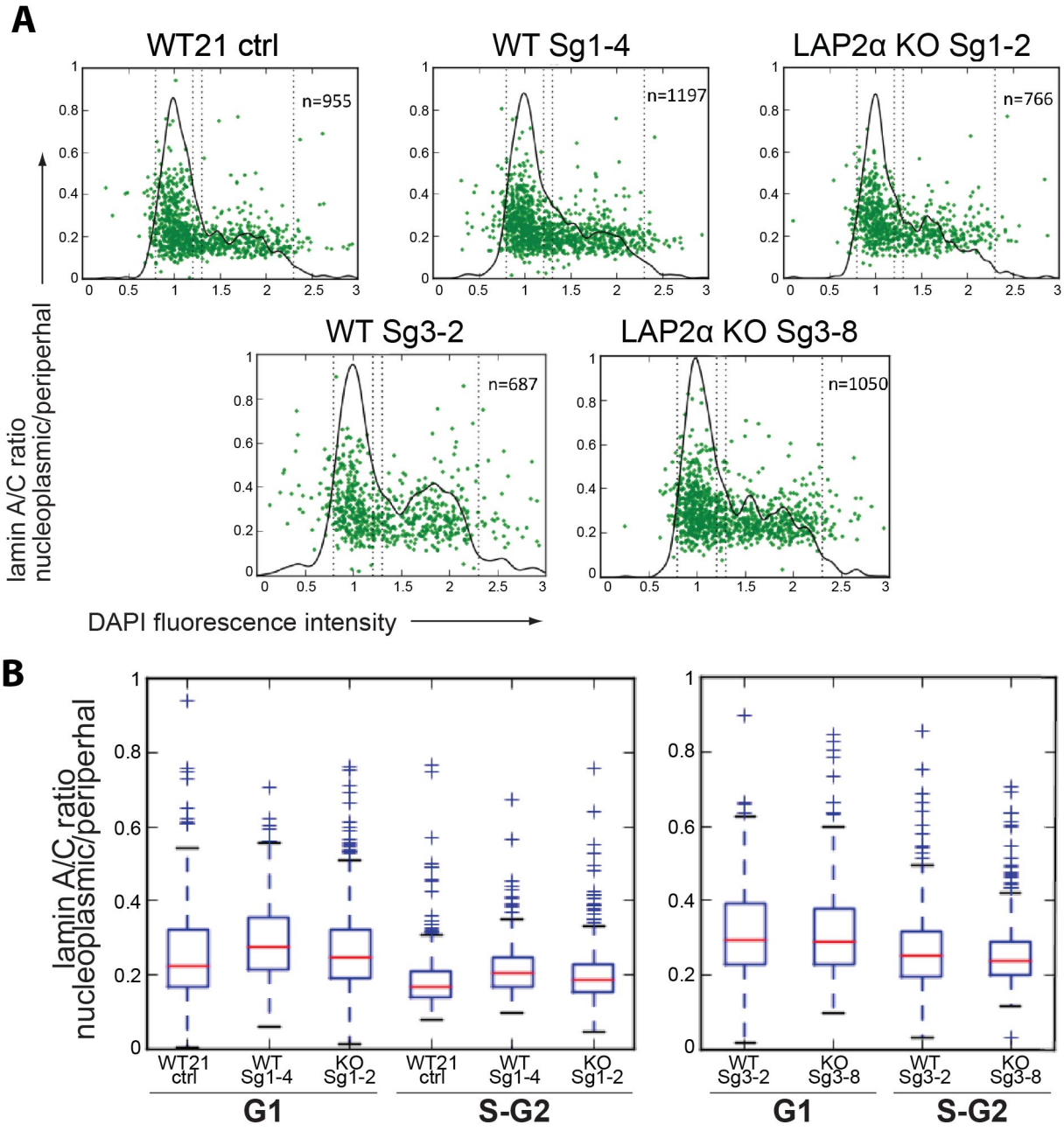

Figure 15. LAP2α does not influence the distribution of mEos3.2 lamin A/C. Signal intensity of DAPI and mEos lamin A/C was measured in wildtype and LAP2α knockout mEos3.2 *LMNA* cells by single cell high throughput analysis. **(A)** Nucleoplasmic to peripheral lamin A/C ratio was calculated for n cells (green dots) and plotted versus DAPI fluorescence intensity, indicating the cell cycle stage. **(B)** Quantification of lamin A/C distribution during G1 and S/G2

phase. Box plots display median values of each clone within the first and third quartiles. Whiskers indicate variability outside the upper and lower quartiles. Individual plus signs indicate outliers.

3.5 Loss of LAP2α might alter the structure of nucleoplasmic A-type lamins

3.5.1 Immunofluorescence reveals LAP2α-dependent fluctuations of nucleoplasmic lamins

In former studies, reduced levels of intranuclear lamin A/C were revealed in LAP2α-deficient cells by immunofluorescence. We were puzzled by the discrepancies between our data and previous findings that had suggested a regulatory role of LAP2α on nucleoplasmic lamins[59]. Thus, we decided to repeat immunofluorescence studies in mEos3.2-*LMNA* cell clones to check for any differences in lamin A/C localization in the absence of LAP2α. We analyzed cells expressing endogenously tagged mEos3.2-lamin A/C at comparable levels in wildtype and LAP2α knockout cells. As depicted in Fig. 16A, we observed that, despite similar levels of intranuclear mEos3.2 lamin A/C, LAP2α-deficient cells exhibit reduced nucleoplasmic lamin A/C antibody staining.

To exclude the possibility that lamin A/C carrying the fluorescent tag behaves differently as untagged lamin A/C, we performed immunofluorescence analysis of cells expressing only mEos3.2 lamin A/C, without any wildtype lamin A/C present (lamin A/C expression shown in Fig. 13D). Cells derived from these clones displayed abnormal nuclear morphology, most likely due to overall reduced expression levels of lamin A/C compared to controls (Fig. 13D), and were not used in other experiments. However, we could still detect a significant reduction in the staining of nucleoplasmic lamins in LAP2α knockout cells (Fig.16B), despite similar levels of nucleoplasmic mEos3.2 lamins A/C, suggesting that the differences observed in WT#21-derived cells are not due to different localization of wildtype untagged and mEos3.2-tagged lamins A/C, but due to different staining properties of nucleoplasmic lamins in LAP2α knockout cells.

Thus, in stark contrast to the results we obtained when investigating the distribution of endogenously tagged lamin A/C by live-cell imaging and fixed cell analysis, indirect immunofluorescence using lamin A/C antibodies shows that lack of LAP2α affects the nucleoplasmic pool of A-type lamins. Considering the discrepancies between our findings, we hypothesized that the reduction of nucleoplasmic lamin antibody staining observed in LAP2α-deficient nuclei might not reflect a real reduction in the levels of intranuclear lamins, but might be due to masking of the epitope recognized by

the lamin A/C antibody specifically in LAP2α-deficient cells. This, in turn, suggests that absence of LAP2α might alter the structure of nucleoplasmic lamins, possibly to a higher assembly state, rendering the epitope located at the N-terminus of lamin A/C inaccessible to the antibody.

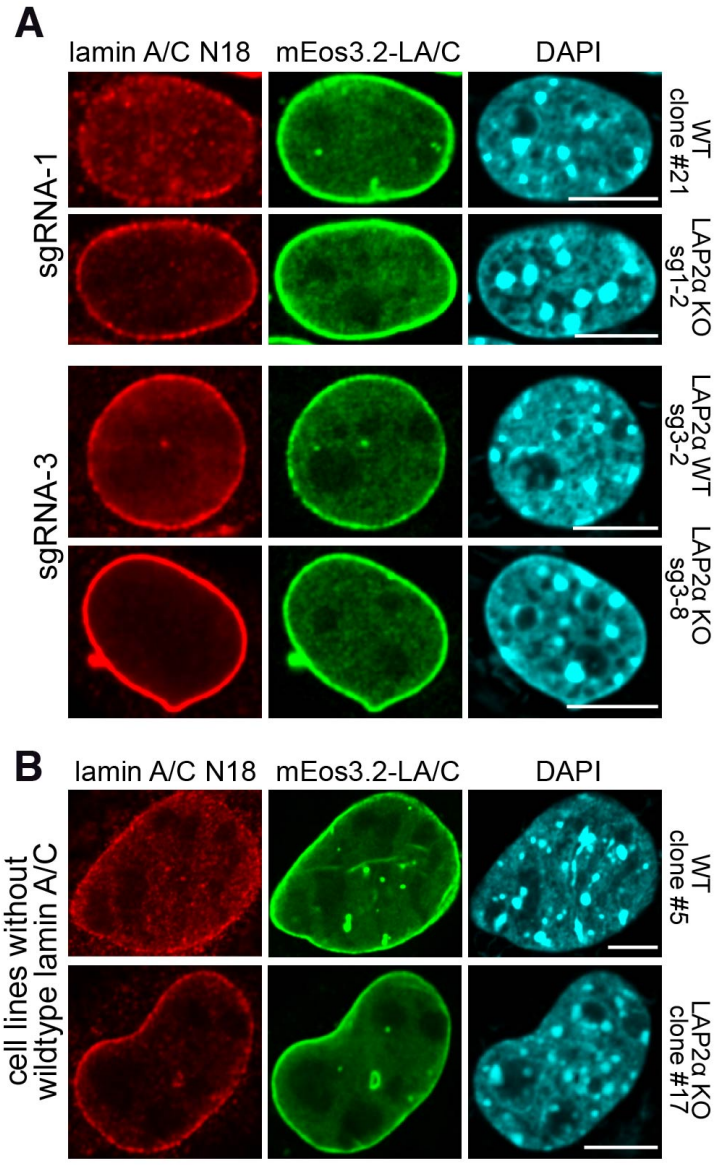

Figure 16. Antibody staining of nucleoplasmic lamins A/C displays differences between LAP2α wildtype and knockout cells. LAP2α wildtype and knockout cells expressing **(A)** both wildtype and mEos3.2 lamin A/C and **(B)** only mEos3.2 lamin A/C were processed for Immunofluorescence analysis using antibodies against lamin A/C (N18) and DAPI to visualize DNA. Confocal images are shown. Bar: 10µm.

3.5.2 Lamin solubility is influenced by the lack of LAP2α

As mentioned in chapter 1.4.1, the structure of intranuclear A-type lamins remains unknown; A-type lamins might reside within the nucleoplasm in the form of short polymers or lamin dimers. We reasoned that if our hypothesis is correct, the altered structure of nucleoplasmic lamins caused by loss of LAP2α would be reflected as a change in the solubility of lamins. Therefore, we performed biochemical extractions of cells deriving from wildtype and LAP2α knockout mEos3.2-LMNA clones and evaluated lamin solubility by Western blot. We found that, using high salt concentration buffer, the soluble fraction of lamins A and C in LAP2α knockout fibroblasts was reduced by approximately 30% compared to wildtype. The reduction was also consistent for mEos3.2 lamins A and C, indicating that lamins carrying the fluorescent tag have similar properties to endogenous lamins (Fig. 17B). The reduced lamin solubility displayed by LAP2α knockout cells supports our hypothesis that lack of LAP2α might alter the structure of nucleoplasmic lamins towards a higher assembly state.

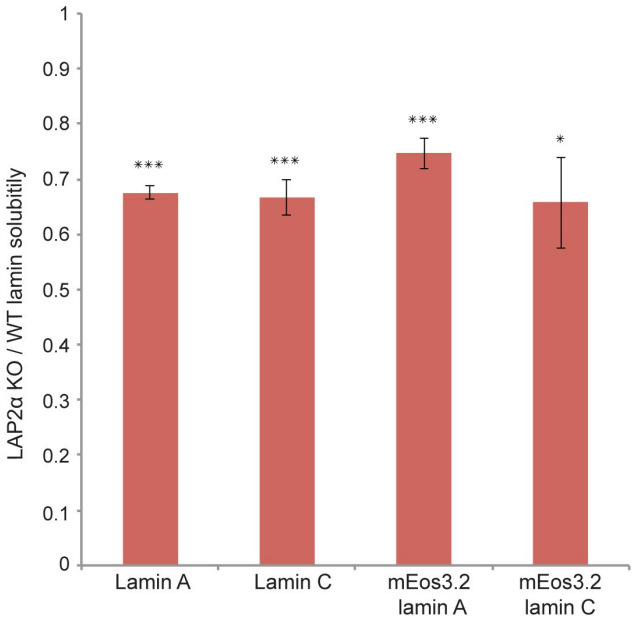

Figure 17. LAP2α-deficient cells display reduced solubility of nucleoplasmic lamins. Evaluation of tagged and untagged lamin A/C solubility based on Western blot quantification. Biochemical extractions were performed using mEos3.2-LMNA LAP2α wildtype and knockout fibroblasts and analyzed by immunoblotting using a mouse monoclonal antibody against lamin A/C. Graph displays the solubility of lamins in LAP2α knockout fibroblast clones relative to wildtype fibroblast clones. Lamin solubility of wildtype clones was arbitrarily set as 1. Solubility

of lamins was normalized to the input (total). Values of individual wildtype (WT, n=3) and LAP2α knockout (KO, n=3) clones were grouped together. Graph shows averages ± standard error ***p<0.0001, *p<0.05 compared to wildtype.

3.6 LAP2α-deficient cells do not display alterations in interphase phosphorylation levels of lamin A/C

Kochin and colleagues[67] showed in 2014 that phosphorylation of lamin A during interphase is involved in the regulation of lamin A localization and function. They identified several interphase phosphorylation sites, two of which were characterized as predominant, since they had the most profound effects on lamin distribution and properties. The authors showed that phosphomimetic mutations on Ser22 and Ser392 resulted in major redistribution of GFP-lamin A towards the nuclear interior, as well as increased mobility. Finally, they found that phosphorylation of lamin A at these sites correlated with increased solubility of both peripheral and nucleoplasmic lamin A.

On account of the link between lamin solubility and phosphorylation during interphase, we proceeded to investigate whether the decreased solubility previously observed in LAP2α knockout is a result of decreased phosphorylation levels of lamin A/C. Cell lysates of LAP2α wildtype and knockout fibrobast clones were analyzed by immunoblotting using antibodies that detect lamin A/C phosphorylated on Ser22 or Ser392 residues (Fig. 18A). We quantified the amount of phosphorylated lamin A/C and did not detect any significant difference between wildtype and LAP2α knockout clones (Fig. 18B).

Subsequently, we studied the levels and distribution of phosphorylated lamin A/C using indirect immunofluorescence. It was possible to perform co-staining of samples with antibodies against LAP2α and pSer22-lamin A/C, and, thus, we our analyzed co-cultures of wildtype and LAP2α knockout cells. However, double staining of samples using antibodies against pSer392-lamin A/C and LAP2α, was impossible due to bleedthrough of fluorescent signal from the red (pSer392-lamin A/C) in the far-red (LAP2α) channel. We believe this occurred due to the very strong signal of the antibody against lamin A/C phosphorylated on Ser392 versus the rather weak signal of the LAP2α antibody. We were, therefore, forced to use individual cultures of wildtype and knockout cells to study Ser392 phosphorylation in this case.

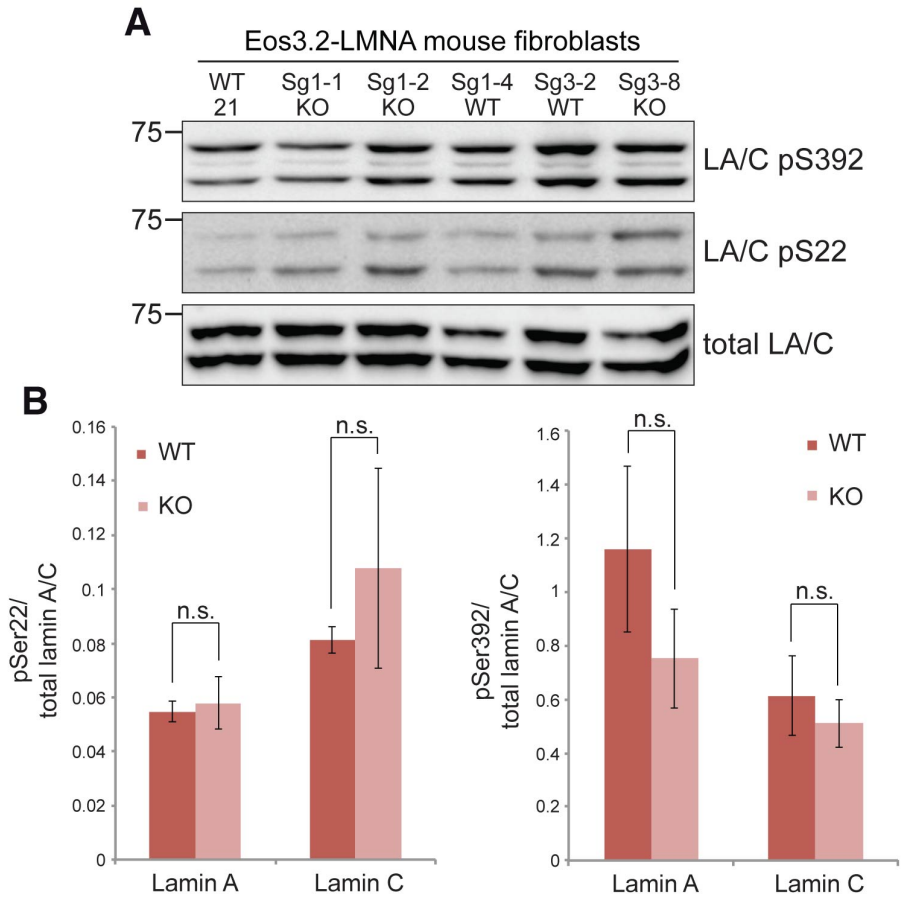

Figure 18. Decreased lamin solubility is not reflected by altered lamin phosphorylation levels in the absence of LAP2α. (A) Cells originating from mEos3.2-LMNA wildtype and LAP2α knockout clones were processed for Western blot analysis using antibodies against the indicated antigens. **(B)** Evaluation of lamin A/C phosphorylation levels by Western blot quantification. The amount of Ser22 and Ser392 phosphorylated lamins was normalized to total lamin A/C. Values of individual wildtype (WT, n= 3) and LAP2α knockout (KO, n= 3) clones were used to calculate the average signal ± standard error. (n.s.: not significant)

Although we did not identify LAP2α-dependent alterations of Ser22 and Ser392 lamin phosphorylation levels (Fig. 19), we made several interesting observations. First, lamin A/C phosphorylated on Ser22 displayed punctate staining in immunofluorescence studies and was exclusively localized in the nuclear interior (Fig. 19A), whereas lamin A/C phosphorylated on Ser392 was found mainly within the nucleoplasm, but also at the nuclear periphery of both LAP2α wildtype and knockout cells (Fig. 19B, left panel). This observation is in line with what was reported so far regarding

the dominant effect of Ser22 phosphorylation on the nucleoplasmic localization of lamin A[67]. On the other hand, phosphorylation of Ser392 does not seem to have such a profound effect on lamin A distribution.

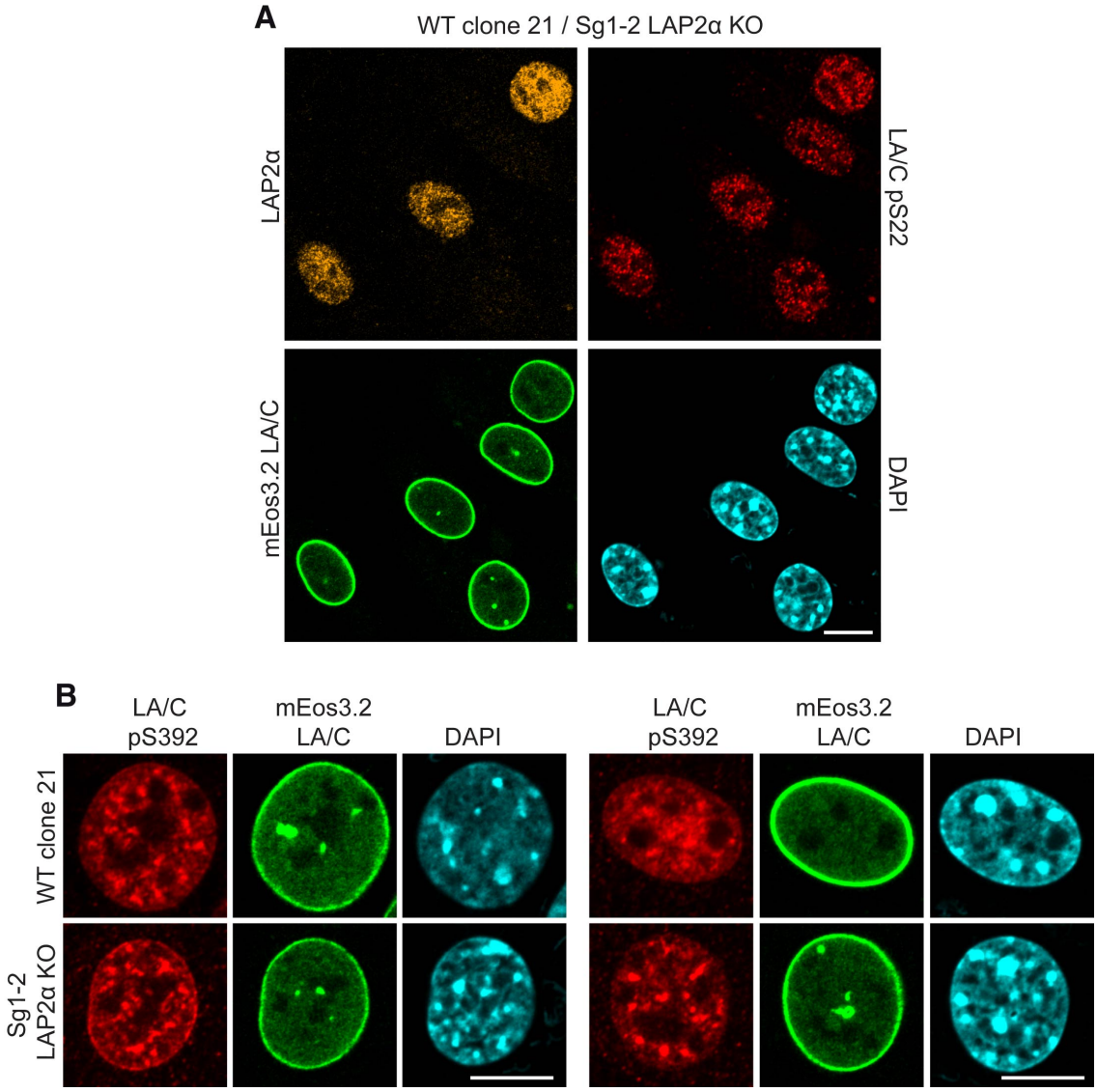

Figure 19. Lamin phosphorylation levels during interphase remain similar between wildtype and LAP2α-deficient cells. Wildtype and LAP2α knockout mEos3.2-LMNA fibroblast clones were processed for immunofluorescence using antibodies against the indicated antigens and DAPI for DNA staining. Representative images used for analysis of **(A)** Ser22 phosphorylation using co-cultures and **(B)** Ser392 phosphorylation using single cultures of wildtype (WT) clone 21 and LAP2α knockout (KO) clone Sg1-2. Bar: 10µm.

Furthermore, we noticed that, while there was no significant change in Ser392 phosphorylation levels, the staining pattern was altered in a fraction of LAP2α knockout cells. In wildtype cells, lamin A/C phosphorylated on Ser392 appeared to form a nucleoplasmic 'veil', similar to the one detected by antibodies against total lamin A/C, with some aggregates (speckles) across the nuclear interior. We observed that, in some LAP2α-deficient cells, this nucleoplasmic staining pattern was altered, appearing more speckled, with more and bigger aggregates, as well as reduced 'veil' staining (Fig. 19B, right panel). How and if the change of staining pattern we observed is relevant to the LAP2α-mediated regulation of nucleoplasmic lamins is not clear from our preliminary experiments and would need to be studied in more detail.

4. Discussion

Nucleoplasmic lamins were long considered to be a transient post-mitotic pool of lamins prior to their integration into the peripheral lamina, or simply a by-product of nuclear lamina dynamics with less, if any, biological significance. However, more recent studies have indicated important novel functions of the nucleoplasmic pool of A-type lamins, distinct from those carried out by the nuclear lamina[56-57]. In the present study, we attempted to gain a better understanding of the origin and dynamics of nucleoplasmic A-type lamins following mitotic cell division, as well as elucidate the regulatory role of LAP2α on intranuclear lamins.

4.1 Origin and dynamics of nucleoplasmic A-type lamins

Regarding the source of intranuclear A-type lamins, it was speculated that the nucleoplasmic lamin pool could originate from more than one cellular pathway[57]. Indeed, when we investigated the newly forming post-mitotic nuclei, we determined two relevant sources significantly contributing to the establishment of a nucleoplasmic pool of A-type lamins (chapter 3.1). We found that, in a cell-cycle linked pathway, a fraction of fully processed mature lamin A, phosphorylated and disassembled during mitosis, is somehow prevented from integrating into the peripheral lamina and localizes within the nuclear interior throughout G1 (Fig. 8A, left). The molecular mechanisms preventing a fraction of lamins from reassembling into the lamina following mitotic cell division and during interphase are not entirely clear. It was suggested that post-translational modifications and/or interactions with lamin-binding proteins are involved in the generation and maintenance of nucleoplasmic A-type lamins in a more soluble and dynamic pool[57] (see also chapter 4.2). Furthermore, we observed that pre-lamin A, which is newly expressed, constitutes an additional source of nucleoplasmic lamins following its maturation (Fig. 8A, right), in this case without the need to go through a mitotic cell division.

Another putative source of nucleoplasmic lamins A/C during interphase may stem from the peripheral lamina, as it has been suggested that there might be a dynamic exchange of lamins between the lamina and the intranuclear lamin pool. While it is interesting to investigate whether this exchange really takes place, in the present study we did not have the means to pursue this further.

Moreover, it is plausible that part of the intranuclear lamin pool also consists of unprocessed pre-lamin A. It has been hypothesized that the non-farnesylated precursor of lamin A briefly localizes to the nuclear interior before being farnesylated and recruited to the periphery[55], where it undergoes further

post-translational modification. However, in our experiments, we could not detect the presence of newly synthesized pre-lamin A in the nuclear interior at the initial time points of imaging. This does not exclude the possibility that the unprocessed form of lamin A transiently localizes to the nuclear interior, since in our experimental setting the protein becomes visible only after maturation of the EGFP fluorophore, which takes approximately 1 hour (see also discussion below). Nevertheless, it is likely that farnesylated lamin A is relatively rapidly recruited to the periphery, or that its levels within the nucleus are too low to be detected. Both explanations suggest that the contribution of unprocessed lamin A to the nucleoplasmic pool of lamins during interphase is probably not significant.

A cascade of post-translational modifications of pre-lamin A is triggered by the presence of a CaaX motif at its C-terminus, which is farnesylated, cleaved, methylated and proteolytically cleaved again[107]. This process gives rise to fully processed mature lamin A, which lacks the final 15aa of pre-lamin A, and, consequently, the farnesyl-group. Disruptions in the post-translational processing of pre-lamin A have been linked to laminopathies, such as progeroid syndromes, lipodystrophy and cardiomyopathy[54, 108-109]. However, genetically engineered mice expressing only mature lamin A do not display any pathology. Apart from the higher occurrence of misshapen fibroblasts, complete lack of pre-lamin A does not seem to cause any major defects. Nevertheless, although it is not entirely clear why, the lamin A processing pathway has been evolutionary conserved[110], providing proof of its functional significance.

Interestingly, using live-cell imaging analysis to monitor newly forming post-mitotic nuclei 'emerging' from the dark (EGFP-tagged lamin variants are expressed only after mitotic cell division, possibly because transfected plasmids cannot enter intact nuclei), we had the opportunity to gain insights into the dynamics of newly synthesized mature and pre-lamin A (chapter 3.2). EGFP-pre-lamin A 'emerges' and remains almost exclusively at the nuclear periphery during early G1 stages and is only detected within the nucleoplasm at later stages (Fig. 8A, right). On the other hand, the dynamics of newly produced mature lamin A in post-mitotic nuclei are inverse (Fig. 8B, left), as it originally resides entirely in the nucleoplasm and progressively assembles into the peripheral lamina. Newly expressed mature lamin A, unlike pre-lamin A, does not undergo the post-translational modifications, indicating that the distinct kinetics we observed are related to lamin A processing. Based on our data, we hypothesize that newly synthesized pre-lamin A, after being imported into the nucleus via its NLS, is rapidly farnesylated and targeted to the INM. There, farnesylated pre-lamin A undergoes further processing to yield the less hydrophobic mature form of lamin A, which is incorporated into the lamina while part of it translocates to the nucleoplasm. The initial localization of newly produced pre-lamin A at the nuclear rim led us to believe that the 'emerging' EGFP-tagged protein is pre-lamin A already carrying

the farnesyl-moiety. Considering that the *in vitro* chromophore maturation time of EGFP is approximately 1 hour[111], it is likely that farnesylation of pre-lamin A precedes the maturation of EGFP. Although the localization of pre-lamin A during this time could not be determined, we speculate that there are two possible scenarios: unprocessed pre-lamin A either localizes to the nuclear periphery immediately after nuclear import, or it resides transiently in the nucleoplasm, where it is farnesylated and targeted to the INM.

Many questions concerning the function of lamin farnesylation remain open. It has mainly been suggested that it facilitates assembly into the lamina[107]. The ability of lamin C, which lacks a CaaX motif, to assemble into the peripheral lamina argues against this hypothesis[51]. Moreover, we show that lamin A expressed in a fully processed form is incorporated normally into the periphery (Fig. 8B, left), providing further proof that integration into the lamina is a farnesylation-independent process. A surprising finding in our study was the detection of newly expressed pre-lamin A-ΔK32 exclusively at the nuclear periphery in early G1, prior to its release into the nucleoplasm (Fig. 8B, middle). Lamin A-ΔK32 is a disease-inducing lamin variant causing severe congenital muscular dystrophy in humans, known to reside entirely in the nucleoplasm[99]. The characteristic lack of a peripheral lamina in *LMNA*$^{\Delta K32/\,\Delta K32}$ cells is attributed to the impaired lateral assembly of head-to-tail polymers into lamin protofilaments. Therefore, detection of pre-lamin A-ΔK32 at the nuclear rim was quite unexpected. However, newly produced mature lamin A-ΔK32 remained nucleoplasmic throughout the imaging course (Fig. 8B, right). Taking into account that only the precursor form of lamin A-ΔK32 transiently localizes to the periphery, we hypothesize that targeting of lamins to the INM is a farnesylation-dependent process, and that farnesylation is sufficient to localize lamins to the periphery, even when they display an assembly defect.

4.2 LAP2α as a regulator of nucleoplasmic lamins

When LAP2α was identified as a regulator of nucleoplasmic lamin levels the effects of its loss were more prominent in G1 cells[59]. Moreover, the most dramatic redistribution of lamins occurs during mitosis and early G1. Thus, we decided to investigate the influence of LAP2α on lamin A/C distribution across the nucleus during cell division and post-mitotic lamina reassembly. We speculated that LAP2α might be involved in retaining a subfraction of lamins in the nucleoplasm after post-mitotic lamina reassembly.

Our first step towards studying the regulation of nucleoplasmic lamins by LAP2α was to monitor the dynamics of mature lamin A in the nuclear interior, originating from the preceding mitosis (chapter

3.3.1), as well as newly synthesized pre-lamin A (chapter 3.3.2). We achieved this by initiating the imaging time course of control and LAP2α-deficient cells after either 24 (matured lamin A) or 5 hours (pre-lamin A), following their transient transfection with EGFP-pre-lamin A. By determining the nucleoplasmic to peripheral lamin A ratio at several time points throughout G1, we found no significant change in the distribution of fully processed mature lamin A and newly synthesized pre-lamin A across the nucleus of LAP2α wildtype and knockout cells (Fig. 9). This finding was quite surprising, as we had previously determined that these two processes contribute to nucleoplasmic lamins (chapter 3.1), and it has been observed in the lab before that the absence of LAP2α reduces nucleoplasmic lamin levels[59, 81]. Lamins originating from the dynamic exchange between the peripheral lamina and nucleoplasmic pool also constitute a putative source of intranuclear lamins[57]. However, it is currently unclear whether such an exchange takes place and, if so, how it might be regulated. Fluorescence recovery after photobleaching (FRAP) experiments have demonstrated that the peripheral lamina is very stable with little dynamic movement[61]. Thus, if there is any exchange with the nucleoplasmic lamin pool, it most likely involves only a minor fraction of peripheral lamins. While such an exchange can still not be excluded, it is technically difficult to investigate and was not further pursued in the current study.

It is still possible that LAP2α is involved in the regulation of this putative exchange between the peripheral lamina and the nucleoplasmic pool. However, since LAP2α depletion causes a significant reduction in the levels of nucleoplasmic lamins as previously described[59, 81], one would expect that the two major sources of lamins in the nuclear interior (mitotic lamins and processed pre-lamin A) would be, among other possible mechanisms, regulated by LAP2α.

Ectopically expressed proteins carrying fluorescent markers are a frequently used tool in microscopic studies. However, protein mislocalization and aggregate formation are just a few of the artifacts reported to be caused by protein overexpression[100]. Hence, we contemplated that perhaps our experimental set-up was the reason that we did not detect any changes in the distribution of nucleoplasmic lamins between LAP2α control and knockout cells. Genetically engineered cell lines generated by integration of a fluorescent marker into the gene locus encoding the protein of interest provide an optimal tool to maintain the innate protein regulation and to study protein properties[112]. For this reason, we used mouse dermal fibroblast clones expressing endogenous lamin A/C fused at the N-terminus to a small fluorophore called mEos3.2 to further investigate the regulatory role of LAP2α on nucleoplasmic lamins. Isogenic mEos3.2-LMNA wildtype and LAP2α-deficient fibroblast clones were generated by Nana Naetar (chapter 3.4.1). Complete characterization of the single cell clones showed that mEos3.2-lamin A/C displayed normal behavior, expression pattern and integration into the lamina

(chapter 3.4.2). Furthermore, cells originating from clones used in further experiments exhibited normal growth rates, as well as cellular and nuclear morphology.

Following the establishment of wildtype and LAP2α knockout fibroblasts clones expressing endogenously labeled lamin A/C, we investigated the effect of LAP2α on endogenous nucleoplasmic A-type lamins. First, live-cell imaging analysis of mEos3.2-lamin A/C dynamics during lamina reassembly in post-mitotic nuclei was performed by Christian Knapp (data not shown). Surprisingly, the distribution of endogenously tagged lamin A/C throughout G1 was similar in control and LAP2α knockout cells and no significant difference in the nucleoplasmic to peripheral ratio of mEos3.2-lamin A/C was found (data not shown). Performing long-term live imaging of single cells is challenging due to phototoxicity and photobleaching issues, data output size and post-acquisition processing, as well as difficulties maintaining the cells within the defined fields of view for a prolonged period of time. Therefore, in this assay, tracking of post-mitotic cells did not extend beyond G1 phase. To study whether LAP2α regulates the distribution of mEos3.2 lamin A/C during different cell cycle stages we performed single cell high throughput analysis of fixed cells originating from control and LAP2α knockout fibroblast clones (chapter 3.4.3). A cell cycle profile was generated based on the DNA content of each cell and plotted against the nucleoplasmic to peripheral lamin A/C ratio (Fig. 15A). Once again, loss of LAP2α did not alter the distribution of lamin A/C across the nucleus in G1 and G2/S phase (Fig. 15B). Nevertheless, immunofluorescence analysis surprisingly confirmed the LAP2α-dependent reduction of nucleoplasmic lamin A/C staining that was previously described, even in cells with similar levels of intranuclear mEos3.2 lamin A/C (chapter 3.5.1).

Thus, data acquired by live-cell imaging analysis of ectopically expressed lamin A and endogenously tagged lamin A/C, as well as fixed cell analysis of mEos3.2 lamin A/C is not compatible with immunofluorescence results and with previous findings showing that absence of LAP2α alters the distribution of lamin A/C across the nucleus[59, 81]. A possible explanation for the discrepancies among our findings is that the reduction of antibody staining within the nucleoplasm of LAP2α-deficient cells is not caused by an actual reduction in nucleoplasmic lamin A/C levels, but rather by antigenic epitope masking. Reduced antibody accessibility could be explained by a change in assembly status and/or structure of nucleoplasmic lamins in the absence of LAP2α. In line with this hypothesis, we show that there is a reduction of approximately 30% in the solubility of both mEos3.2 and wildtype lamin A/C in cells depleted off LAP2α (chapter 3.5.2). Extraction of the nuclei was performed under conditions, where the peripheral lamina should mainly remain insoluble. Therefore, it is likely that the decreased lamin solubility we observed is, primarily, due to changes inflicted on lamins in the nucleoplasm. More

evidence suggesting an altered assembly status of nucleoplasmic lamins in the absence of LAP2α arose from the characterization of nucleoplasmic lamin mobility in living cells performed by Yuval Garini and his lab at Bar-Ilan University, Israel. Mobility of intranuclear lamins was determined using continuous fluorescence photobleaching (CP)[113], where fluorescent lamin molecules (GFP-lamin A and mEos3.2 lamin A/C) were continuously bleached by moderate illumination in randomly selected small regions within the nucleoplasm. CP was performed on cells transiently expressing GFP-lamin A, as well as cells constitutively expressing endogenous mEos3.2 lamin A/C and based on the bleaching and recovery by diffusion rates, the dynamics of nucleoplasmic lamins were determined. Cells depleted of LAP2α displayed a significant reduction in lamin mobility of both ectopic lamin A and tagged endogenous lamin A/C residing in the nucleoplasm (Y. Garini and I. Bronshtein, personal communication, data not shown).

Altogether, the aforementioned results regarding the role of LAP2α in nucleoplasmic lamin regulation led us to revise the previously described model suggesting that LAP2α influences the amount of nucleoplasmic A-type lamins[86]. Instead, we hypothesize that LAP2α is involved in maintaining the nucleoplasmic pool of A-type lamins in a low-assembly, mobile state (Fig. 20). LAP2α-depletion-dependent changes of intranuclear lamin A/C structure towards a higher assembly state could explain why our initial experiments showed similar levels of nucleoplasmic lamins in control and LAP2α knockout cells, while immunofluorescence studies showed a clear reduction in nucleoplasmic lamin levels in the absence of LAP2α, probably due to reduced antibody accessibility (epitope masking). The reduced mobility and solubility of lamin A/C in the nuclear interior in LAP2α knockout cells also supports this hypothesis. To date, the structural organization of intranuclear lamins remains poorly understood. Data obtained using electron microscopy originally suggested the presence of lamin filaments, not only at the nuclear periphery, but throughout the nucleoplasm[58]. However, more recent studies showing that lamin A/C forms a highly mobile[60, 63, 98] and easily extractable[59, 64] lamin pool in the nuclear interior, suggest a low assembly state of nucleoplasmic A-type lamins.

One can only speculate about the mechanism by which LAP2α maintains the nucleoplasmic A-type lamin pool in a mobile and soluble state. One possible scenario is that LAP2α interferes with the formation of higher assembly lamin filaments solely by binding to the C-terminal domain of nucleoplasmic A-type lamins. Alternatively, the interaction between LAP2α and lamin A/C could regulate the assembly state of nucleoplasmic lamins by influencing the post-translational modifications of lamin molecules, e.g. phosphorylation[57]. Kochin et al[67] suggested a link between increased lamin solubility and mobility and interphase phosphorylation of A-type lamins, specifically at serine residues located at positions 22 and 392. Our analysis, however, did not reveal any significant difference in the

phosphorylation levels of these residues between LAP2α wildtype and knockout fibroblast clones (chapter 3.6), suggesting that LAP2α alters the properties of nucleoplasmic lamins in a phosphorylation-independent manner.

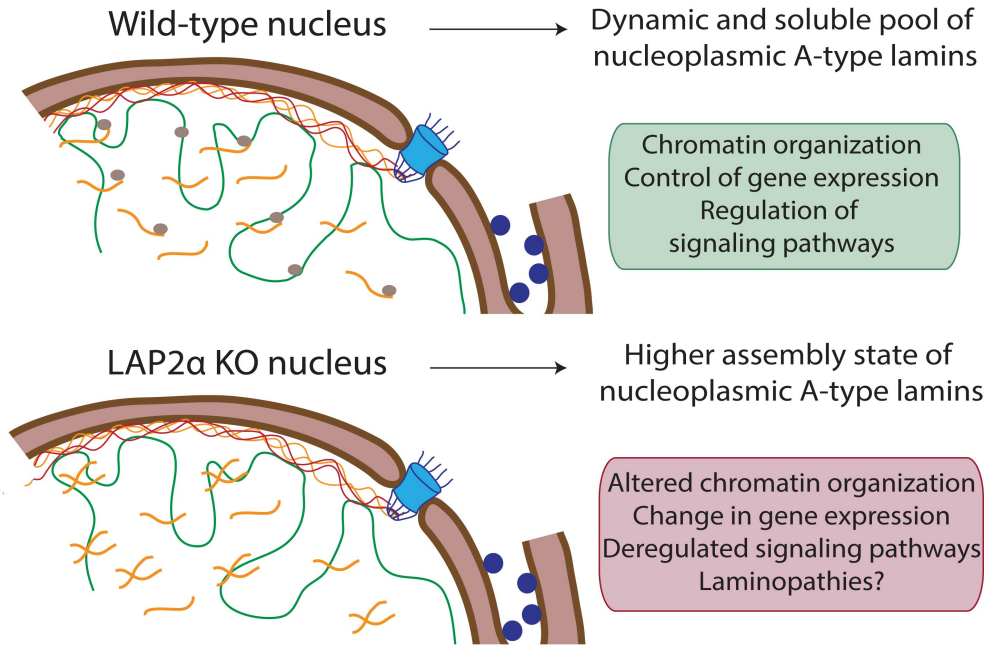

Figure 20. Schematic representation of nucleoplasmic A-type lamins of wildtype and LAP2α knockout cells. Loss of LAP2α possibly changes the structure of nucleoplasmic lamins towards a higher assembly state. Our data suggests that, contrary to what was proposed previously, LAP2α does not regulate the level of lamin A/C within the nucleoplasm, but rather maintains A-type lamins in a more dynamic and soluble state in the nuclear interior.

The nuclear lamina is involved in several cellular processes and its importance for maintaining the cellular homeostasis is apparent by the numerous defects caused by mutations in genes encoding its major components, lamins[114]. More recent studies have implicated the nucleoplasmic pool of A-type lamins in important functions, such as chromatin organization[81], promoter accessibility, nuclear mechanical response[57] and pRb-mediated signaling[86, 115]. Moreover, certain defects evoked by disease-causing mutations in *LMNA* are linked to the redistribution of lamin A/C across the nucleus, either towards the nucleoplasm (*LMNA* ΔK32, *LMNA* N195K), or the periphery (*LMNA* G608G-progerin)[57]. Based on data we acquired during this study, we propose that LAP2α alters the polymerization state of nucleoplasmic A-type lamins. This, in turn, could affect binding of intranuclear A-type lamins to binding

partners (e.g. pRb, transcription factors and other signaling molecules), as well as chromatin. In line with this hypothesis, it was suggested that the loss of equilibrium between proliferation and differentiation (skewed towards proliferation) displayed by stem and progenitor cells of LAP2α-deficient mice is caused by altered pRb activity[59]. Considering that pRb-mediated signaling has been identified as one of the signaling pathways affected in lamin-linked diseases[116], the influence of A-type lamin-LAP2α complexes on pRb activity could be relevant to laminopathy phenotypes. Furthermore, it was shown that proliferation defects of progeria cells, which down-regulate LAP2α expression and lose the nucleoplasmic pool of A-type lamins, can be rescued upon re-expression of LAP2α, possibly by regulation of chromatin and expression of extracellular matrix genes[117].

In the present study, we addressed the regulatory role of LAP2α on nucleoplasmic lamins. We provide data that led us to question the former hypothesis claiming that LAP2α influences the levels of A-type lamins in the nuclear interior, and instead, we speculated that LAP2α might alter the assembly state of nucleoplasmic A-type lamins. Elucidating the mechanism of action of LAP2α is highly relevant for a better understanding of the regulation of nucleoplasmic A-type lamins. Given the increasing evidence of functions specific to the nucleoplasmic lamin pool, understanding its regulation is crucial to decipher its potential contribution to fundamental cellular processes and lamin-linked diseases.

5. References

1. Alberts Bruce, J. A., Lewis Julian, Morgan David, Raff Martin, Roberts Keith, Walter Peter, *Molecular biology of the cell*. 6th ed.; Garland Science: 2015.
2. Görlich, D.; Kutay, U., Transport Between the Cell Nucleus and the Cytoplasm. *Annual Review of Cell and Developmental Biology* **1999,** *15* (1), 607-660.
3. Dahl, K. N.; Kalinowski, A., Nucleoskeleton mechanics at a glance. *Journal of Cell Science* **2011,** *124* (5), 675-678.
4. Osmanagic-Myers, S.; Dechat, T.; Foisner, R., Lamins at the crossroads of mechanosignaling. *Genes Dev* **2015,** *29* (3), 225-37.
5. Cavalli, G.; Misteli, T., Functional implications of genome topology. *Nature structural & molecular biology* **2013,** *20* (3), 290-9.
6. Sexton, T.; Cavalli, G., The role of chromosome domains in shaping the functional genome. *Cell* **2015,** *160* (6), 1049-59.
7. Dixon, J. R.; Selvaraj, S.; Yue, F.; Kim, A.; Li, Y.; Shen, Y.; Hu, M.; Liu, J. S.; Ren, B., Topological domains in mammalian genomes identified by analysis of chromatin interactions. *Nature* **2012,** *485* (7398), 376-80.
8. Lupiáñez, D. G.; Spielmann, M.; Mundlos, S., Breaking TADs: How Alterations of Chromatin Domains Result in Disease. *Trends in Genetics* **2016,** *32* (4), 225-237.
9. Hetzer, M. W.; Walther, T. C.; Mattaj, I. W., PUSHING THE ENVELOPE: Structure, Function, and Dynamics of the Nuclear Periphery. *Annual Review of Cell and Developmental Biology* **2005,** *21* (1), 347-380.
10. Gerace, L.; Burke, B., Functional Organization of the Nuclear Envelope. *Annual Review of Cell Biology* **1988,** *4* (1), 335-374.
11. Worman, H. J.; Ostlund, C.; Wang, Y., Diseases of the nuclear envelope. *Cold Spring Harbor perspectives in biology* **2010,** *2* (2), a000760.
12. Burke, B.; Stewart, C. L., Life at the edge: the nuclear envelope and human disease. *Nature reviews. Molecular cell biology* **2002,** *3* (8), 575-85.
13. Kabachinski, G.; Schwartz, T. U., The nuclear pore complex – structure and function at a glance. *Journal of Cell Science* **2015,** *128* (3), 423-429.
14. Strambio-De-Castillia, C.; Niepel, M.; Rout, M. P., The nuclear pore complex: bridging nuclear transport and gene regulation. *Nature reviews. Molecular cell biology* **2010,** *11* (7), 490-501.
15. Fawcett, D. W., On the occurrence of a fibrous lamina on the inner aspect of the nuclear envelope in certain cells of vertebrates. *American Journal of Anatomy* **1966,** *119* (1), 129-145.
16. Gruenbaum, Y.; Foisner, R., Lamins: nuclear intermediate filament proteins with fundamental functions in nuclear mechanics and genome regulation. *Annu Rev Biochem* **2015,** *84*, 131-64.
17. Gerace, L.; Huber, M. D., Nuclear lamina at the crossroads of the cytoplasm and nucleus. *J Struct Biol* **2012,** *177* (1), 24-31.
18. de Leeuw, R.; Gruenbaum, Y.; Medalia, O., Nuclear Lamins: Thin Filaments with Major Functions. *Trends in cell biology* **2018,** *28* (1), 34-45.
19. Burke, B.; Stewart, C. L., The nuclear lamins: flexibility in function. *Nature reviews. Molecular cell biology* **2013,** *14* (1), 13-24.
20. Stuurman, N.; Heins, S.; Aebi, U., Nuclear Lamins: Their Structure, Assembly, and Interactions. *Journal of Structural Biology* **1998,** *122* (1), 42-66.
21. Herrmann, H.; Aebi, U., Intermediate Filaments: Structure and Assembly. *Cold Spring Harbor perspectives in biology* **2016,** *8* (11).
22. Peter, A.; Stick, R., Evolution of the lamin protein family: what introns can tell. *Nucleus (Austin, Tex.)* **2012,** *3* (1), 44-59.

23. Butin-Israeli, V.; Adam, S. A.; Goldman, A. E.; Goldman, R. D., Nuclear lamin functions and disease. *Trends in Genetics* **2012,** *28* (9), 464-471.
24. Dittmer, T. A.; Misteli, T., The lamin protein family. *Genome biology* **2011,** *12* (5), 222.
25. Lin, F.; Worman, H. J., Structural organization of the human gene encoding nuclear lamin A and nuclear lamin C. *The Journal of biological chemistry* **1993,** *268* (22), 16321-6.
26. Dechat, T.; Adam, S. A.; Taimen, P.; Shimi, T.; Goldman, R. D., Nuclear lamins. *Cold Spring Harbor perspectives in biology* **2010,** *2* (11), a000547.
27. Wilson, K. L.; Foisner, R., Lamin-binding Proteins. *Cold Spring Harbor perspectives in biology* **2010,** *2* (4), a000554.
28. Schirmer, E. C.; Foisner, R., Proteins that associate with lamins: many faces, many functions. *Experimental cell research* **2007,** *313* (10), 2167-79.
29. de Las Heras, J. I.; Meinke, P.; Batrakou, D. G.; Srsen, V.; Zuleger, N.; Kerr, A. R.; Schirmer, E. C., Tissue specificity in the nuclear envelope supports its functional complexity. *Nucleus (Austin, Tex.)* **2013,** *4* (6), 460-77.
30. Olins, A. L.; Rhodes, G.; Welch, D. B.; Zwerger, M.; Olins, D. E., Lamin B receptor: multi-tasking at the nuclear envelope. *Nucleus (Austin, Tex.)* **2010,** *1* (1), 53-70.
31. Barton, L. J.; Soshnev, A. A.; Geyer, P. K., Networking in the nucleus: a spotlight on LEM-domain proteins. *Current Opinion in Cell Biology* **2015,** *34*, 1-8.
32. Gruenbaum, Y.; Aebi, U., Intermediate filaments: a dynamic network that controls cell mechanics. *F1000prime reports* **2014,** *6*, 54.
33. McKeon, F. D.; Kirschner, M. W.; Caput, D., Homologies in both primary and secondary structure between nuclear envelope and intermediate filament proteins. *Nature* **1986,** *319* (6053), 463-8.
34. Fisher, D. Z.; Chaudhary, N.; Blobel, G., cDNA sequencing of nuclear lamins A and C reveals primary and secondary structural homology to intermediate filament proteins. *Proceedings of the National Academy of Sciences* **1986,** *83* (17), 6450-6454.
35. Parry, D. A.; Conway, J. F.; Steinert, P. M., Structural studies on lamin. Similarities and differences between lamin and intermediate-filament proteins. *The Biochemical journal* **1986,** *238* (1), 305-8.
36. Dhe-Paganon, S.; Werner, E. D.; Chi, Y. I.; Shoelson, S. E., Structure of the globular tail of nuclear lamin. *The Journal of biological chemistry* **2002,** *277* (20), 17381-4.
37. Krimm, I.; Ostlund, C.; Gilquin, B.; Couprie, J.; Hossenlopp, P.; Mornon, J. P.; Bonne, G.; Courvalin, J. C.; Worman, H. J.; Zinn-Justin, S., The Ig-like structure of the C-terminal domain of lamin A/C, mutated in muscular dystrophies, cardiomyopathy, and partial lipodystrophy. *Structure (London, England : 1993)* **2002,** *10* (6), 811-23.
38. Loewinger, L.; McKeon, F., Mutations in the nuclear lamin proteins resulting in their aberrant assembly in the cytoplasm. *The EMBO journal* **1988,** *7* (8), 2301-2309.
39. Ben-Harush, K.; Wiesel, N.; Frenkiel-Krispin, D.; Moeller, D.; Soreq, E.; Aebi, U.; Herrmann, H.; Gruenbaum, Y.; Medalia, O., The Supramolecular Organization of the C. elegans Nuclear Lamin Filament. *Journal of Molecular Biology* **2009,** *386* (5), 1392-1402.
40. Aebi, U.; Cohn, J.; Buhle, L.; Gerace, L., The nuclear lamina is a meshwork of intermediate-type filaments. *Nature* **1986,** *323* (6088), 560-4.
41. Grossman, E.; Dahan, I.; Stick, R.; Goldberg, M. W.; Gruenbaum, Y.; Medalia, O., Filaments assembly of ectopically expressed Caenorhabditis elegans lamin within Xenopus oocytes. *Journal of Structural Biology* **2012,** *177* (1), 113-118.
42. Harapin, J.; Bormel, M.; Sapra, K. T.; Brunner, D.; Kaech, A.; Medalia, O., Structural analysis of multicellular organisms with cryo-electron tomography. *Nature methods* **2015,** *12* (7), 634-6.
43. Shimi, T.; Kittisopikul, M.; Tran, J.; Goldman, A. E.; Adam, S. A.; Zheng, Y.; Jaqaman, K.; Goldman, R. D., Structural organization of nuclear lamins A, C, B1, and B2 revealed by superresolution microscopy. *Molecular biology of the cell* **2015,** *26* (22), 4075-86.

44. Xie, W.; Chojnowski, A.; Boudier, T.; Lim, John S. Y.; Ahmed, S.; Ser, Z.; Stewart, C.; Burke, B., A-type Lamins Form Distinct Filamentous Networks with Differential Nuclear Pore Complex Associations. *Current Biology* **2016,** *26* (19), 2651-2658.
45. Turgay, Y.; Eibauer, M.; Goldman, A. E.; Shimi, T.; Khayat, M.; Ben-Harush, K.; Dubrovsky-Gaupp, A.; Sapra, K. T.; Goldman, R. D.; Medalia, O., The molecular architecture of lamins in somatic cells. *Nature* **2017,** *543* (7644), 261-264.
46. Rusinol, A. E.; Sinensky, M. S., Farnesylated lamins, progeroid syndromes and farnesyl transferase inhibitors. *J Cell Sci* **2006,** *119* (Pt 16), 3265-72.
47. Dechat, T.; Pfleghaar, K.; Sengupta, K.; Shimi, T.; Shumaker, D. K.; Solimando, L.; Goldman, R. D., Nuclear lamins: major factors in the structural organization and function of the nucleus and chromatin. *Genes Dev* **2008,** *22* (7), 832-53.
48. Sinensky, M.; Fantle, K.; Trujillo, M.; McLain, T.; Kupfer, A.; Dalton, M., The processing pathway of prelamin A. *J Cell Sci* **1994,** *107 (Pt 1)*, 61-7.
49. Kitten, G. T.; Nigg, E. A., The CaaX motif is required for isoprenylation, carboxyl methylation, and nuclear membrane association of lamin B2. *J Cell Biol* **1991,** *113* (1), 13-23.
50. Corrigan, D. P.; Kuszczak, D.; Rusinol, A. E.; Thewke, D. P.; Hrycyna, C. A.; Michaelis, S.; Sinensky, M. S., Prelamin A endoproteolytic processing in vitro by recombinant Zmpste24. *The Biochemical journal* **2005,** *387* (Pt 1), 129-38.
51. Fong, L. G.; Ng, J. K.; Lammerding, J.; Vickers, T. A.; Meta, M.; Cote, N.; Gavino, B.; Qiao, X.; Chang, S. Y.; Young, S. R.; Yang, S. H.; Stewart, C. L.; Lee, R. T.; Bennett, C. F.; Bergo, M. O.; Young, S. G., Prelamin A and lamin A appear to be dispensable in the nuclear lamina. *The Journal of clinical investigation* **2006,** *116* (3), 743-52.
52. Adam, S. A.; Butin-Israeli, V.; Cleland, M. M.; Shimi, T.; Goldman, R. D., Disruption of lamin B1 and lamin B2 processing and localization by farnesyltransferase inhibitors. *Nucleus (Austin, Tex.)* **2013,** *4* (2), 142-50.
53. Sasseville, A. M.; Raymond, Y., Lamin A precursor is localized to intranuclear foci. *J Cell Sci* **1995,** *108 (Pt 1)*, 273-85.
54. Casasola, A.; Scalzo, D.; Nandakumar, V.; Halow, J.; Recillas-Targa, F.; Groudine, M.; Rincon-Arano, H., Prelamin A processing, accumulation and distribution in normal cells and laminopathy disorders. *Nucleus (Austin, Tex.)* **2016,** *7* (1), 84-102.
55. Barrowman, J.; Hamblet, C.; George, C. M.; Michaelis, S., Analysis of prelamin A biogenesis reveals the nucleus to be a CaaX processing compartment. *Molecular biology of the cell* **2008,** *19* (12), 5398-408.
56. Dechat, T.; Gesson, K.; Foisner, R., Lamina-independent lamins in the nuclear interior serve important functions. *Cold Spring Harb Symp Quant Biol* **2010,** *75*, 533-43.
57. Naetar, N.; Ferraioli, S.; Foisner, R., Lamins in the nuclear interior - life outside the lamina. *J Cell Sci* **2017,** *130* (13), 2087-2096.
58. Hozak, P.; Sasseville, A. M.; Raymond, Y.; Cook, P. R., Lamin proteins form an internal nucleoskeleton as well as a peripheral lamina in human cells. *Journal of Cell Science* **1995,** *108* (2), 635-644.
59. Naetar, N.; Korbei, B.; Kozlov, S.; Kerenyi, M. A.; Dorner, D.; Kral, R.; Gotic, I.; Fuchs, P.; Cohen, T. V.; Bittner, R.; Stewart, C. L.; Foisner, R., Loss of nucleoplasmic LAP2alpha-lamin A complexes causes erythroid and epidermal progenitor hyperproliferation. *Nat Cell Biol* **2008,** *10* (11), 1341-8.
60. Shimi, T.; Pfleghaar, K.; Kojima, S.; Pack, C. G.; Solovei, I.; Goldman, A. E.; Adam, S. A.; Shumaker, D. K.; Kinjo, M.; Cremer, T.; Goldman, R. D., The A- and B-type nuclear lamin networks: microdomains involved in chromatin organization and transcription. *Genes Dev* **2008,** *22* (24), 3409-21.
61. Broers, J. L.; Machiels, B. M.; van Eys, G. J.; Kuijpers, H. J.; Manders, E. M.; van Driel, R.; Ramaekers, F. C., Dynamics of the nuclear lamina as monitored by GFP-tagged A-type lamins. *Journal of Cell Science* **1999,** *112* (20), 3463-3475.

62. Moir, R. D.; Yoon, M.; Khuon, S.; Goldman, R. D., Nuclear Lamins a and B1. *Different Pathways of Assembly during Nuclear Envelope Formation in Living Cells* **2000,** *151* (6), 1155-1168.
63. Bronshtein, I.; Kepten, E.; Kanter, I.; Berezin, S.; Lindner, M.; Redwood, A. B.; Mai, S.; Gonzalo, S.; Foisner, R.; Shav-Tal, Y.; Garini, Y., Loss of lamin A function increases chromatin dynamics in the nuclear interior. *Nature communications* **2015,** *6*, 8044.
64. Kolb, T.; Maass, K.; Hergt, M.; Aebi, U.; Herrmann, H., Lamin A and lamin C form homodimers and coexist in higher complex forms both in the nucleoplasmic fraction and in the lamina of cultured human cells. *Nucleus (Austin, Tex.)* **2011,** *2* (5), 425-33.
65. Simon, D. N.; Wilson, K. L., Partners and post-translational modifications of nuclear lamins. *Chromosoma* **2013,** *122* (1-2), 13-31.
66. Heald, R.; McKeon, F., Mutations of phosphorylation sites in lamin A that prevent nuclear lamina disassembly in mitosis. *Cell* **1990,** *61* (4), 579-89.
67. Kochin, V.; Shimi, T.; Torvaldson, E.; Adam, S. A.; Goldman, A.; Pack, C. G.; Melo-Cardenas, J.; Imanishi, S. Y.; Goldman, R. D.; Eriksson, J. E., Interphase phosphorylation of lamin A. *J Cell Sci* **2014,** *127* (Pt 12), 2683-96.
68. Zhang, Y.-Q.; Sarge, K. D., Sumoylation regulates lamin A function and is lost in lamin A mutants associated with familial cardiomyopathies. *The Journal of Cell Biology* **2008,** *182* (1), 35-39.
69. Dechat, T.; Korbei, B.; Vaughan, O. A.; Vlcek, S.; Hutchison, C. J.; Foisner, R., Lamina-associated polypeptide 2alpha binds intranuclear A-type lamins. *Journal of Cell Science* **2000,** *113* (19), 3473-3484.
70. Gerace, L.; Blobel, G., The nuclear envelope lamina is reversibly depolymerized during mitosis. *Cell* **1980,** *19* (1), 277-87.
71. Kuga, T.; Nozaki, N.; Matsushita, K.; Nomura, F.; Tomonaga, T., Phosphorylation statuses at different residues of lamin B2, B1, and A/C dynamically and independently change throughout the cell cycle. *Experimental cell research* **2010,** *316* (14), 2301-12.
72. Dechat, T.; Gajewski, A.; Korbei, B.; Gerlich, D.; Daigle, N.; Haraguchi, T.; Furukawa, K.; Ellenberg, J.; Foisner, R., LAP2α and BAF transiently localize to telomeres and specific regions on chromatin during nuclear assembly. *Journal of Cell Science* **2004,** *117* (25), 6117-6128.
73. Dechat, T.; Shimi, T.; Adam, S. A.; Rusinol, A. E.; Andres, D. A.; Spielmann, H. P.; Sinensky, M. S.; Goldman, R. D., Alterations in mitosis and cell cycle progression caused by a mutant lamin A known to accelerate human aging. *Proceedings of the National Academy of Sciences* **2007,** *104* (12), 4955-4960.
74. Berger, R.; Theodor, L.; Shoham, J.; Gokkel, E.; Brok-Simoni, F.; Avraham, K. B.; Copeland, N. G.; Jenkins, N. A.; Rechavi, G.; Simon, A. J., The characterization and localization of the mouse thymopoietin/lamina-associated polypeptide 2 gene and its alternatively spliced products. *Genome research* **1996,** *6* (5), 361-70.
75. Wagner, N.; Krohne, G., LEM-Domain proteins: new insights into lamin-interacting proteins. *International review of cytology* **2007,** *261*, 1-46.
76. Brachner, A.; Foisner, R., Evolvement of LEM proteins as chromatin tethers at the nuclear periphery. *Biochemical Society transactions* **2011,** *39* (6), 1735-41.
77. Dechat, T.; Vlcek, S.; Foisner, R., Review: lamina-associated polypeptide 2 isoforms and related proteins in cell cycle-dependent nuclear structure dynamics. *J Struct Biol* **2000,** *129* (2-3), 335-45.
78. Dechat, T.; Gotzmann, J.; Stockinger, A.; Harris, C. A.; Talle, M. A.; Siekierka, J. J.; Foisner, R., Detergent-salt resistance of LAP2alpha in interphase nuclei and phosphorylation-dependent association with chromosomes early in nuclear assembly implies functions in nuclear structure dynamics. *The EMBO journal* **1998,** *17* (16), 4887-902.
79. Dorner, D.; Vlcek, S.; Foeger, N.; Gajewski, A.; Makolm, C.; Gotzmann, J.; Hutchison, C. J.; Foisner, R., Lamina-associated polypeptide 2alpha regulates cell cycle progression and differentiation via the retinoblastoma-E2F pathway. *J Cell Biol* **2006,** *173* (1), 83-93.

80. Bradley, C. M.; Jones, S.; Huang, Y.; Suzuki, Y.; Kvaratskhelia, M.; Hickman, A. B.; Craigie, R.; Dyda, F., Structural basis for dimerization of LAP2alpha, a component of the nuclear lamina. *Structure (London, England : 1993)* **2007,** *15* (6), 643-53.
81. Gesson, K.; Rescheneder, P.; Skoruppa, M. P.; von Haeseler, A.; Dechat, T.; Foisner, R., A-type lamins bind both hetero- and euchromatin, the latter being regulated by lamina-associated polypeptide 2 alpha. *Genome research* **2016,** *26* (4), 462-73.
82. Lund, E.; Collas, P., Nuclear lamins: making contacts with promoters. *Nucleus (Austin, Tex.)* **2013,** *4* (6), 424-30.
83. Shimi, T.; Butin-Israeli, V.; Adam, S. A.; Goldman, R. D., Nuclear lamins in cell regulation and disease. *Cold Spring Harb Symp Quant Biol* **2010,** *75*, 525-31.
84. Vlcek, S.; Korbei, B.; Foisner, R., Distinct functions of the unique C terminus of LAP2alpha in cell proliferation and nuclear assembly. *The Journal of biological chemistry* **2002,** *277* (21), 18898-907.
85. Gajewski, A.; Csaszar, E.; Foisner, R., A phosphorylation cluster in the chromatin-binding region regulates chromosome association of LAP2alpha. *The Journal of biological chemistry* **2004,** *279* (34), 35813-21.
86. Naetar, N.; Foisner, R., Lamin complexes in the nuclear interior control progenitor cell proliferation and tissue homeostasis. *Cell cycle (Georgetown, Tex.)* **2009,** *8* (10), 1488-93.
87. Weinberg, R. A., The retinoblastoma protein and cell cycle control. *Cell* **1995,** *81* (3), 323-30.
88. Johnson, B. R.; Nitta, R. T.; Frock, R. L.; Mounkes, L.; Barbie, D. A.; Stewart, C. L.; Harlow, E.; Kennedy, B. K., A-type lamins regulate retinoblastoma protein function by promoting subnuclear localization and preventing proteasomal degradation. *Proceedings of the National Academy of Sciences of the United States of America* **2004,** *101* (26), 9677-82.
89. Van Berlo, J. H.; Voncken, J. W.; Kubben, N.; Broers, J. L.; Duisters, R.; van Leeuwen, R. E.; Crijns, H. J.; Ramaekers, F. C.; Hutchison, C. J.; Pinto, Y. M., A-type lamins are essential for TGF-beta1 induced PP2A to dephosphorylate transcription factors. *Human molecular genetics* **2005,** *14* (19), 2839-49.
90. Rodriguez, J.; Calvo, F.; Gonzalez, J. M.; Casar, B.; Andres, V.; Crespo, P., ERK1/2 MAP kinases promote cell cycle entry by rapid, kinase-independent disruption of retinoblastoma-lamin A complexes. *J Cell Biol* **2010,** *191* (5), 967-79.
91. Schreiber, K. H.; Kennedy, B. K., When lamins go bad: nuclear structure and disease. *Cell* **2013,** *152* (6), 1365-75.
92. Broers, J. L.; Ramaekers, F. C.; Bonne, G.; Yaou, R. B.; Hutchison, C. J., Nuclear lamins: laminopathies and their role in premature ageing. *Physiological reviews* **2006,** *86* (3), 967-1008.
93. Janin, A.; Bauer, D.; Ratti, F.; Millat, G.; Mejat, A., Nuclear envelopathies: a complex LINC between nuclear envelope and pathology. *Orphanet journal of rare diseases* **2017,** *12* (1), 147.
94. Hutchison, C. J.; Alvarez-Reyes, M.; Vaughan, O. A., Lamins in disease: why do ubiquitously expressed nuclear envelope proteins give rise to tissue-specific disease phenotypes? *J Cell Sci* **2001,** *114* (Pt 1), 9-19.
95. Mariappan, I.; Parnaik, V. K., Sequestration of pRb by cyclin D3 causes intranuclear reorganization of lamin A/C during muscle cell differentiation. *Molecular biology of the cell* **2005,** *16* (4), 1948-60.
96. Gotzmann, J.; Foisner, R., A-type lamin complexes and regenerative potential: a step towards understanding laminopathic diseases? *Histochem Cell Biol* **2006,** *125* (1-2), 33-41.
97. Zhang, M.; Chang, H.; Zhang, Y.; Yu, J.; Wu, L.; Ji, W.; Chen, J.; Liu, B.; Lu, J.; Liu, Y.; Zhang, J.; Xu, P.; Xu, T., Rational design of true monomeric and bright photoactivatable fluorescent proteins. *Nature methods* **2012,** *9* (7), 727-9.
98. Moir, R. D.; Yoon, M.; Khuon, S.; Goldman, R. D., Nuclear lamins A and B1: different pathways of assembly during nuclear envelope formation in living cells. *J Cell Biol* **2000,** *151* (6), 1155-68.
99. Bertrand, A. T.; Renou, L.; Papadopoulos, A.; Beuvin, M.; Lacene, E.; Massart, C.; Ottolenghi, C.; Decostre, V.; Maron, S.; Schlossarek, S.; Cattin, M. E.; Carrier, L.; Malissen, M.; Arimura, T.; Bonne,

G., DelK32-lamin A/C has abnormal location and induces incomplete tissue maturation and severe metabolic defects leading to premature death. *Human molecular genetics* **2012,** *21* (5), 1037-48.
100. Gibson, T. J.; Seiler, M.; Veitia, R. A., The transience of transient overexpression. *Nature methods* **2013,** *10* (8), 715-21.
101. Ran, F. A.; Hsu, P. D.; Wright, J.; Agarwala, V.; Scott, D. A.; Zhang, F., Genome engineering using the CRISPR-Cas9 system. *Nature protocols* **2013,** *8* (11), 2281-2308.
102. Hsu, Patrick D.; Lander, Eric S.; Zhang, F., Development and Applications of CRISPR-Cas9 for Genome Engineering. *Cell* **2014,** *157* (6), 1262-1278.
103. Sander, J. D.; Joung, J. K., CRISPR-Cas systems for editing, regulating and targeting genomes. *Nature biotechnology* **2014,** *32* (4), 347-55.
104. Wiedenmann, J.; Nienhaus, G. U., Live-cell imaging with EosFP and other photoactivatable marker proteins of the GFP family. *Expert review of proteomics* **2006,** *3* (3), 361-74.
105. Lykke-Andersen, S.; Jensen, T. H., Nonsense-mediated mRNA decay: an intricate machinery that shapes transcriptomes. *Nature reviews. Molecular cell biology* **2015,** *16* (11), 665-77.
106. Roukos, V.; Pegoraro, G.; Voss, T. C.; Misteli, T., Cell cycle staging of individual cells by fluorescence microscopy. *Nature protocols* **2015,** *10* (2), 334-48.
107. Davies, B. S. J.; Coffinier, C.; Yang, S. H.; Barnes, R. H.; Jung, H.-J.; Young, S. G.; Fong, L. G., Investigating the purpose of prelamin A processing. *Nucleus (Austin, Tex.)* **2011,** *2* (1), 4-9.
108. Davies, B. S.; Fong, L. G.; Yang, S. H.; Coffinier, C.; Young, S. G., The posttranslational processing of prelamin A and disease. *Annual review of genomics and human genetics* **2009,** *10*, 153-74.
109. Capanni, C.; Mattioli, E.; Columbaro, M.; Lucarelli, E.; Parnaik, V. K.; Novelli, G.; Wehnert, M.; Cenni, V.; Maraldi, N. M.; Squarzoni, S.; Lattanzi, G., Altered pre-lamin A processing is a common mechanism leading to lipodystrophy. *Human molecular genetics* **2005,** *14* (11), 1489-502.
110. Beck, L. A.; Hosick, T. J.; Sinensky, M., Isoprenylation is required for the processing of the lamin A precursor. *J Cell Biol* **1990,** *110* (5), 1489-99.
111. Sniegowski, J. A.; Lappe, J. W.; Patel, H. N.; Huffman, H. A.; Wachter, R. M., Base catalysis of chromophore formation in Arg96 and Glu222 variants of green fluorescent protein. *The Journal of biological chemistry* **2005,** *280* (28), 26248-55.
112. Ratz, M.; Testa, I.; Hell, S. W.; Jakobs, S., CRISPR/Cas9-mediated endogenous protein tagging for RESOLFT super-resolution microscopy of living human cells. *Scientific reports* **2015,** *5*, 9592.
113. Wachsmuth, M.; Weidemann, T.; Muller, G.; Hoffmann-Rohrer, U. W.; Knoch, T. A.; Waldeck, W.; Langowski, J., Analyzing intracellular binding and diffusion with continuous fluorescence photobleaching. *Biophysical journal* **2003,** *84* (5), 3353-63.
114. Dobrzynska, A.; Gonzalo, S.; Shanahan, C.; Askjaer, P., The nuclear lamina in health and disease. *Nucleus (Austin, Tex.)* **2016,** *7* (3), 233-48.
115. Andres, V.; Gonzalez, J. M., Role of A-type lamins in signaling, transcription, and chromatin organization. *J Cell Biol* **2009,** *187* (7), 945-57.
116. Maraldi, N. M.; Capanni, C.; Cenni, V.; Fini, M.; Lattanzi, G., Laminopathies and lamin-associated signaling pathways. *Journal of cellular biochemistry* **2011,** *112* (4), 979-92.
117. Vidak, S.; Kubben, N.; Dechat, T.; Foisner, R., Proliferation of progeria cells is enhanced by lamina-associated polypeptide 2α (LAP2α) through expression of extracellular matrix proteins. *Genes Dev* **2015,** *29* (19), 2022-36.